

A THEORETICAL INVESTIGATION OF THE NUCLEAR
RESONANCE ABSORPTION SPECTRUM OF SPODUMENE

GILLES LAMARCHE

A Thesis submitted in partial fulfilment of the
requirements for the degree of

Master of Arts

in the

Department of Physics

We accept this thesis as conforming to the standard
required for the degree of Master of Arts

Members of the Department of Physics

The University of British Columbia

April, 1953

ABSTRACT

The interaction of nuclei of spin $I > \frac{1}{2}$ and non-vanishing quadrupole moment with their surroundings in a crystal consists of two parts: magnetic and electrostatic. In the absence of any external field, the interaction is mainly the quadrupole interaction of the nuclei with the electric field gradient of the crystal, since the crystalline magnetic field is often small and contributes only to the broadening of the quadrupole lines. When an external magnetic field is added, a Zeeman effect is introduced and both interactions are present at the same time.

In this thesis a study is made of the resonance absorption spectrum of a nucleus subjected to both fields when the ratio of the two interaction energies assumes any given arbitrary value.

After a brief survey of the theory of both interactions, and the various perturbation approximations, the problem for a nucleus of spin $I = 5/2$ is stated explicitly and a brief analysis shows that the solution is particularly simple in the cases where the external magnetic field coincides with one of the principal axes of the electric field gradient. For other directions of the magnetic field, the problem cannot be simplified in any obvious way and leads to much longer numerical calculations.

The problem is completely solved numerically in a special case for Al^{27} in a spodumene crystal for one particular crystal orientation, but over the entire experimentally interesting range of the external magnetic field so as to fit directly the conditions of an experiment proposed in Dr. Volkoff's laboratory in order to aid in the evaluation of its feasibility. The expected variation of the frequencies and the relative intensities of the resonance lines as a function of the applied magnetic field is exhibited in a series of graphs.

ACKNOWLEDGMENTS

The author wishes to express his gratitude to Dr. G. M. Volkoff for suggesting the problem and guiding this thesis through numerous discussions and comments.

He also wants to thank him and the other members of the Department who through lectures and discussions have increased his knowledge of and enthusiasm for Physics.

L'auteur tient aussi a remercier Le Ministere du Bien Etre Social et de la Jeunesse de la Province de Quebec pour une genereuse bourse qui lui a permis de poursuivre ses etudes pendant deux annees consecutives au Departement de Physique de l'Universite de la Colombie Britannique.

TABLE OF CONTENTS

ABSTRACT	i
ACKNOWLEDGMENTS	iii
INTRODUCTION	1
SECTION I: PURE QUADRUPOLE SPECTRA	8
A. Case of axial symmetry	9
B. Case of no symmetry	12
SECTION II: SPECTRA DUE TO COMBINED QUADRUPOLE AND ZEEMAN INTERACTIONS	16
A. Pure Zeeman Effect	16
B. Small Zeeman perturbation on the quadrupole spectra	16
C. Small Quadrupole perturbation on the Zeeman effect	20
SECTION III: EQUALLY STRONG QUADRUPOLE AND ZEEMAN INTERACTIONS	22
A. Secular determinant for the case $I = 5/2$	22
B. Case of $\theta = 0^\circ$	26
C. Other orientations of the magnetic field \vec{H}	38
SUMMARY AND CONCLUSION	42
REFERENCES	43

LIST OF FIGURES

Fig. 1	Dependence on the asymmetry parameter of the energy levels of the nucleus in the "pure quadrupole case" facing page	14
--------	---	----

Fig. 2	Energy levels for the case $I = 5/2$, $\eta = 0$ and the magnetic field in the direction of the z-axis, as a function of H , facing page	18
Fig. 3	Energy levels for the special case $I = 5/2$, $\eta = 0.95$ and $\theta = 0^\circ$ as a function of R , facing page	28
Fig. 4	Square of the coefficients of the eigenfunctions for the eigenvalues of fig. 3 Group L, facing page	29
Fig. 5	The same as fig. 4 for the group M, facing page	29
Fig. 6	Transition frequencies for the special case of fig. 3 as a function of R , facing page	32
Fig. 7	Square of the matrix elements (arbitrary scale) as a function of R , facing page	34
Fig. 8	Energy levels for the case $I = 5/2$, $\eta = 0.95$ and $\theta = 90^\circ$ (field along the x-axis) as a function of R , facing page	39

LIST OF TABLES

TABLE I :	Transition frequencies (in Mc/sec) and squares of the matrix elements (arbitrary units) for $0 \leq R \leq 4$, at intervals of $R = 0.4$	36
TABLE II:	Frequencies of the Zeeman lines obtained by a quadrupole interaction perturbation theory compared with the frequencies calculated directly for the special case of $I = 5/2$, $\eta = 0.95$, $\theta = 0^\circ$, and quadrupole constant $C_z = 2.96$ Mc/sec, for $R = 2, 4, 8$ and 20	37
TABLE III:	Squares of the coefficients of the eigenfunctions for the case of the magnetic field along the x-axis and $R = 6$	40

INTRODUCTION

The study of nuclear resonance absorption lines in crystals gives information about both nuclei and crystals. The properties of the nuclei to be obtained are the spin I , the magnetic moment $\vec{\mu}$ and the electric quadrupole moment eQ . With regard to crystals this method gives information on the electric field gradient which is closely related to the symmetry properties of crystalline structure (C2, T1, C3), on relaxation mechanism (B2, B3, P3, P4, P5, W2) and also on the position of special nuclei (A2, I1, P1).

Analysis of the various spectra obtained is valuable to chemists (A1, D1, L2, M1), Townes and Dailey (T1) discuss some of the implications of the results obtained by this method for the theory of chemical binding.

Much work has been done in this field during the last few years. Here we will attempt only a brief survey of that part of the field in which the present thesis lies.

In crystals investigated by nuclear resonance methods, we have to deal with two general kinds of interactions of nuclei with their surroundings: magnetic and electrostatic interactions.

Magnetic interactions. Nuclei with spin $I \neq 0$ possess a magnetic dipole $\mu = g \beta \vec{I}$, where g is the gyromagnetic ratio of the nucleus and β the nuclear magneton. The nuclear dipoles in the presence of a magnetic field will assume a

finite number of orientations corresponding to definite energy levels. The magnetic fields to be considered are external magnetic fields to which the crystal is subjected in experiments, and magnetic fields produced in the crystals themselves.

The energy levels of a magnetic dipole in the presence of a uniform magnetic field \vec{H} only are the equidistant Zeeman energy levels giving rise to a unique transition frequency $\nu_0 = \frac{\mu H}{h}$, formed by the superposition of transitions between adjacent levels according to the selection rule $\Delta m = \pm 1$.

Usually in a crystal, at the site of the nucleus, other magnetic fields are also present. These are due to the presence of neighboring dipoles. In some cases this field turns out to be quite strong and well oriented, as when two (P1), three (A2), four (I1) protons are present in a closely spaced, well defined group and interact with each other. The net result is a splitting of the single Zeeman transition line into many components, since the energy levels are perturbed and no longer equidistant. But on top of this effect, and even when this strong interaction exists, the other nuclear dipoles distributed in the crystal create at the site of the nucleus under consideration a weak but non-negligible magnetic field. Since the macroscopic effect to be observed depends on a great number of similar nuclei in analogous positions in each unit cell, and since the microscopic fields can vary from one cell to another because of the varying contributions of the other dipoles, the line or

lines are broadened (V1). The effect of these two different internal magnetic fields usually appears as a perturbation on the Zeeman effect and can be called respectively "structure" and "diffuse" perturbation.

Electrostatic Interactions. On the other hand crystalline structure exposes nuclei to microscopic inhomogeneous electric fields, repeated in each unit cell, that cannot be produced in the laboratory. If these nuclei are not electrically of spherical symmetry, they possess an electric quadrupole moment eQ , which interact with the gradient of the electric field.

The energy of interaction will depend on the orientation of the nucleus giving rise to a finite number of quadrupole levels that the nuclear resonance methods can detect, provided the spacing between these levels exceeds the line width due to magnetic dipole-dipole interaction mentioned above. Transitions between energy levels resulting from this interaction alone have been observed in cases where the field gradient does or does not possess an axial symmetry. The theory has been given by Kruger (K1), Bersohn (B1). Many results can be found in Kruger (K1), Dehmelt and Kruger (D3-D4), Kruger and Meyer-Berkhot (K2, K3), Dean (D2), Livingstone (L1). From these results one can obtain the value of the quadrupole coupling constant $\frac{eQ\varphi_{zz}}{h}$ where φ_{zz} is the largest eigenvalue of the tensor when this tensor is taken in an ^{axes system} ~~direction~~ in which it is diagonal, and the asymmetry parameter η .

When the splitting between the quadrupole levels

is comparable to the dipole-dipole interaction, the quadrupole interaction will merely contribute to the line broadening. This effect has been considered by Bersohn. In polycrystalline samples where all unit cells are not oriented in the same direction but randomly distributed the transition lines are broadened. Even in single crystals, the field experienced by similarly situated nuclei may vary from cell to cell due to crystal imperfections and impurities and the lines are also broadened by this diffuse perturbation effect.

Magnetic and Electric Interaction

If we subject to an external magnetic field a crystal in which there is an electric quadrupole interaction, the Zeeman levels will be perturbed, and the single Zeeman line will be split into many components. According to the ratio of the Zeeman and quadrupole energy, either effect can become a perturbation on the other.

At one extreme we have the case where the magnetic interaction of each dipole with an external magnetic field produces Zeeman levels separated by energies quite large compared to the splitting due to quadrupole interaction of the nucleus with its surroundings. In these instances, the quadrupole interaction is taken as a perturbation on the Zeeman effect. This perturbation theory giving information on the perturbed energy levels, and the transition lines from which the quadrupole coupling constant, the orientation, and asymmetry of the field gradient may be

obtained, has received much attention. Carr and Kikuchi (C1) have obtained an expression for the frequencies to the first order in the ratio $\frac{eQq_{zz}}{\mu H_0}$. Pound (P6) extended it to the third order in case of axially symmetric field, and this theory has been further extended to case of asymmetry by Bersohn (B1) and Volkoff et al (V2, V3).

At the other extreme, Dehmelt and Kruger (K1, D7) have investigated theoretically and experimentally the pure quadrupole case and have obtained information on the quadrupole coupling constant in case of axially symmetric crystals. The theory was then extended to non symmetric crystalline field gradient by Kruger (K1) and observations^{were} published by Dehmelt and Kruger (D6, D3, D4, D5) giving the value of quadrupole coupling constant as well as the degree of asymmetry of the field. Bersohn (B1) gives a general expression for the perturbation in terms of an axial asymmetry parameter up to the fourth order.

The introduction of a weak external magnetic field can be treated as a perturbation on the pure quadrupole levels. Kruger (K1) obtained a first order expansion in terms of the magnetic field strength. Observation of this effect is reported by Kruger and Meyer-Berkhout (K3) and Dean (D2). Bersohn (B1) has calculated also a second order perturbation.

As the external magnetic field is increased the perturbation theory from this side breaks down while the perturbation theory where the quadrupole interaction energy appears as

a perturbation on the magnetic levels is not yet valid. The object of our thesis is first to give a brief description of, and then to link together the two extreme regions and to show that a complete knowledge of the energy levels, and the frequencies and intensities of transitions between them can be obtained by a direct numerical solution of the secular determinant. Unfortunately this method of solution can not be carried out with much generality. Our method is somewhat similar to the one used by Weiss(W3) for the study of the paramagnetic resonance spectrum of Chromic Alums. In our discussion we will disregard completely the diffuse perturbation, magnetic and electrostatic, giving rise to broadening of the lines.

The purpose of obtaining the information on the dependence of the transition frequencies and intensities on the external magnetic field strength is to aid in the evaluation of the feasibility of a proposed experiment of observing the resonance absorption spectrum of Al^{27} in spodumene over a complete range of values of the magnetic field showing the gradual transition from a pure quadrupole spectrum to the other extreme of a single Zeeman line split into a number of closely spaced components. Such an experiment will yield no further new information on nuclei or on crystals which cannot be obtained by experiments in the ranges of H where one or the other perturbation theory is valid, but it will serve as a contribution to the field of resonance spectroscopy.

We also compare the exact solution with a perturbation expansion, showing the limit of validity of the latter.

In section I we review briefly the principal aspects of the pure quadrupole interaction both in the presence and absence of axial symmetry of the field. In section II, the introduction of an external magnetic field is discussed. In section III, we obtain an explicit form for the secular determinant for the case of $I = 5/2$. We solve this determinant for the particular case of the external magnetic field applied in the direction of one of the principal axes of the \sqrt{E} crystal. We then calculate the transition frequencies and their relative intensities, and present the information in graphical form. We also discuss briefly the case of the magnetic field along the two other principal axes giving an explicit example.

We conclude that the problem leads to a simple solution only if the external magnetic field is along one of these axes. Other cases require larger amount of numerical work.

I. PURE QUADRUPOLE SPECTRA

To obtain an expression for the energy of interaction of the nuclear electric quadrupole moment with the gradient of the electric field of the crystal, one must find first an expression for the general electrostatic interaction energy of the system. Then it is possible to isolate from it the quadrupole term F . This has been done previously (C2, P5) and here we will quote only the results necessary for our calculations.

F can be written as a complete scalar product of two tensors:

$$F = \tilde{Q} \cdot \tilde{\nabla} E \quad (1)$$

Where \tilde{Q} is the nuclear quadrupole tensor, and $\tilde{\nabla} E$ the electric field gradient tensor of the crystal taken at the site of the nucleus. Using the methods of group theory, it is possible to write both tensors in terms of their irreducible components.

The irreducible components of the quadrupole moment tensor involve a single scalar eQ and the angular momentum operators.

The $\tilde{\nabla} E$ tensor may be expressed in terms of the second derivatives of φ , the electric potential. Then the matrix elements of F are easily found. The scalar nuclear quadrupole moment eQ is defined in the conventional manner in the $1m_2$ representation by: $(11 | \sum_i e_i r_i^2 (3 \cos^2 \theta_{iX}) | 11)$ where the nuclear charge e_i is at a distance r_i from the origin and makes with the direction of quantization of \hat{I} , and angle θ_{iX} . For our purposes, it is sufficient to write $\tilde{\nabla} E$ in its simple diagonal form. This is

possible since the tensor is symmetric ($\frac{\partial^2}{\partial x \partial y} = \frac{\partial^2}{\partial y \partial x}$, etc.) and this in turn guarantees that a set of axes x, y, z , can be found to put this tensor in its diagonal form. These axes x, y, z , are called the principal axes of the field gradient tensor, and in this system the irreducible components of ∇E are simply:

$$\begin{aligned} (\nabla E)_0 &= \frac{1}{2} \varphi_{33} \\ (\nabla E)_{\pm 1} &= 0 \\ (\nabla E)_{\pm 2} &= \frac{\sqrt{6}}{12} (\varphi_{xx} - \varphi_{yy}) \end{aligned} \quad (2)$$

where φ_{33} for instance is the second derivative of the electrostatic potential φ with respect to z taken at the site of the nucleus.

In this particular case the energy operator can be written as:

$$F = \frac{eQ}{4I(2I-1)} \left[(3\vec{I}_z^2 - \vec{I}^2) \varphi_{33} + (\vec{I}_x^2 - \vec{I}_y^2) (\varphi_{xx} - \varphi_{yy}) \right] \quad (3)$$

Where \vec{I} is the angular momentum operator whose matrix elements in the $I m_I$ representation are well known.

Except when otherwise stated I will always be understood to be some odd multiple of $\frac{1}{2}h$. When I is an even multiple of $\frac{1}{2}h$, the discussion is slightly different (W1).

A. Case of Axial Symmetry.

The electric field at the site of a given nucleus in a crystal depends on all the charges outside the nucleus: valence electrons, inner core of electrons, and ions at a distance of an atomic radius or more from the nucleus in question (T1).

In many cases the main contribution to the field gradient (which decreases as the inverse cube of the distance) is from the atoms forming the unit cell around the nucleus under consideration, so that geometrical consideration of their charges help in predicting the nature of the field gradient. The simplest case of interest is when the field gradient is axially symmetrical (the case of spherical symmetry is of no interest since then all components of $\vec{\nabla}E$ are zero). A good example of a practical case is $Bn(CH_3)$ (K1) at the site of Br, the symmetry axis passing through Br and C. Here F has a particularly simple form since $\varphi_{xx} = \varphi_{yy} = -\frac{1}{2}\varphi_{zz}$ if we remember that $\nabla \cdot \vec{E} = 0$ at the position occupied by the nucleus. Then the operator is:

$$F_s = \frac{eQ\varphi_{zz}}{4I(2I-1)} (3\hat{I}_z^2 - \hat{I}^2) \quad (4)$$

In the $I m_3$ representation F_s is diagonal and the energy eigenvalues are the diagonal elements:

$$E_{m_3} = (m_3 | F | m_3) = \frac{eQ\varphi_{zz}}{4I(2I-1)} [3m_3^2 - I(I+1)] \quad (5)$$

$E_{m_3} = E_{-m_3}$ and each level is doubly degenerate and belongs to two eigenfunctions: ψ_{m_3} and ψ_{-m_3} . $I \pm \frac{1}{2}$ transitions can be induced between the $I \pm \frac{1}{2}$ adjacent levels. If we agree to take $m_3 > 0$, then the allowed magnetic transitions $m_3 \rightarrow m_3 - 1$ have frequencies

$$\nu_{m_3 \rightarrow m_3 - 1} = \frac{3eQ\varphi_{zz}}{4I(2I-1)} (2m_3 - 1), \quad m_3 = \frac{3}{2}, \frac{5}{2}, \frac{7}{2}, \dots \quad (6)$$

which for $m_3 = \frac{3}{2}, \frac{5}{2}, \frac{7}{2}, \dots$ are in the ratio 1:2:3:...

If the complete spectrum can be obtained in a particular case, the number of levels will give I , while $\frac{eQ\varphi_{zz}}{h}$ the quadrupole constant can be easily obtained from the knowledge

of the values of the transitions frequencies. The quadrupole constant involving the quadrupole moment and the biggest component in absolute value of the field gradient of the crystal is characteristic of a particular nucleus at a well defined site in a given crystal.

Let us note at once that the ν 's are independent of the angle γ that the r.f. magnetic field \vec{H}_1 used to detect them, makes with the z-axis of the gradient. The intensity of the spectral lines on the contrary varies as $\sin^2 \gamma$, enabling us to determine experimentally the direction of the z axis. Cohen (C2) has given an expression for the transition probability. We will reproduce it showing how it is derived.

The intensity of transition lines between state m and state m' is proportional to the square of the absolute value of the matrix element mm' of the time dependent perturbing operator \mathcal{H}_p . Let the angular frequency of the rotating field H_1 be ω . The energy operator is:

$$\mathcal{H}_p = -g\beta \vec{H}_1 \cdot \vec{I} = -g\beta [H_x \vec{I}_x + H_y \vec{I}_y + H_z \vec{I}_z] \quad (7)$$

For an oscillating field $H_1 \cos \omega t$ lying in the xz plane and making an angle γ with respect to the z-axis, we have:

$$H_x = H_1 \sin \gamma \cos \omega t \quad (8)$$

$$H_y = 0$$

$$H_z = H_1 \cos \gamma \cos \omega t$$

\mathcal{H}_p can then be rewritten as:

$$\mathcal{H}_p = -g\beta H_1 \cos \omega t \sin \gamma [(\vec{I}_x + i\vec{I}_y) + (\vec{I}_x - i\vec{I}_y)] - \\ - g\beta H_1 \cos \omega t \cos \gamma \vec{I}_z \quad (9)$$

when ω is near the transition frequency between two adjacent energy levels we will have induced transitions if $|m_3 - m'_3| = 1$.

The square of the $(m_3, m_3 - 1)$ -matrix elements are:

$$|(m_3 | \mathcal{H}_p | m_3 - 1)|^2 = \frac{1}{4} g^2 \beta^2 H_1^2 \sin^2 \gamma [I(I-1) - m_3(m_3 - 1)] \quad (10)$$

and the intensity will be proportional to this term. The intensity is then expected to decrease as $|m_3|$ increases.

Since the intensity of spectral lines is proportional to $\sin^2 \gamma$, two rotations will be necessary to locate the z axis. The first arbitrary rotation will indicate by its minimum a plane in which the z axis lies. A second rotation around an axis perpendicular to this plane will give the direction of the z axis at zero intensity.

B. Case of No Symmetry

In cases where the structure of the crystal is such that the electric field gradient does not show any symmetry, it is useful to describe its departure from axial symmetry by means of an asymmetry parameter η . Taking the largest component in absolute value of the diagonal tensor as $\phi_{33} = eq$, now $\phi_{xx} \neq \phi_{yy}$ and the directions of the x and y principal axes are no more arbitrary. It is useful to express them all in terms of the scalar eq and to define $\phi_{xx} = \frac{-eq(1-\eta)}{2}$, from which it follows that

$\phi_{yy} = \frac{-eq(1+\eta)}{2}$. The parameter η is then defined by

$$\eta = \frac{\phi_{xx} - \phi_{yy}}{\phi_{33}} \quad (11)$$

From equation (3)

$$F_A = \frac{e^2 g Q}{4I(2I-1)} [(3\vec{I}_3^2 - \vec{I}^2) + (\vec{I}_x^2 - \vec{I}_y^2)\eta] \quad (12)$$

with the non-zero matrix elements in the I, m_3 representation:

$$(m_3 | F_A | m_3) = \frac{e^2 g Q}{4I(2I-1)} [3m_3^2 - I(I+1)] \quad (13)$$

$$(m_3 | F_A | m_3 \pm 2) = \frac{e^2 g Q}{4I(2I-1)} f^{1/2}(I, m_3 \pm 1)$$

$$\text{where } f(I, m_3) = \frac{1}{4} (I - m_3 + 1)(I + m_3)(I - m_3)(I + m_3 + 1)$$

The eigenvalues are obtained by the solution of the secular determinant:

$$|F_{A m_3 m_3'} - E \delta_{m_3 m_3'}| = 0 \quad (14)$$

For any given $I > \frac{1}{2}$ the determinant can be rearranged, leading to the problem of solving two equivalent equations of degree $I + \frac{1}{2}$. The eigenfunctions belonging to each degenerate eigenvalue are no longer linear combinations of only two functions ψ_{m_3} and $\psi_{m_3'}$ as in the case of axial symmetry, but of all the angular momentum eigenfunctions of the representation. The double Kramers degeneracy is not removed by the introduction of the axial asymmetry when I is an odd multiple of $\frac{1}{2}\hbar$, and so the eigenfunction belonging to each eigenvalue appears as any linear combination of two sets of functions themselves given as linear combination of $I + \frac{1}{2}$ angular momentum eigenfunctions. The right linear combination of the two sets can be found to fit continuously when the degeneracy is removed by some magnetic field.

Perturbation calculations can be carried out when the departure from axial symmetry is small, ie. when $\eta \ll 1$.

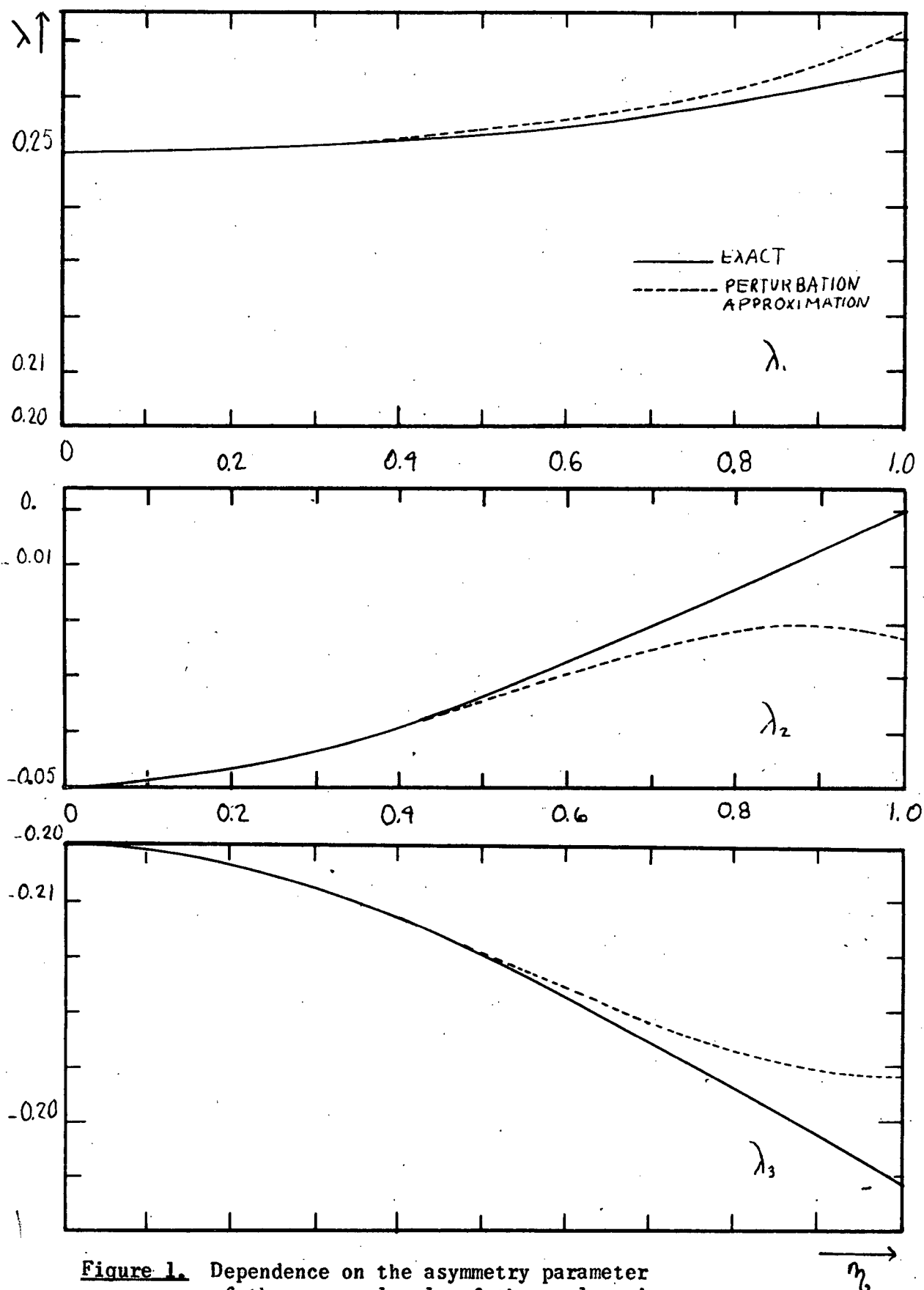


Figure 1. Dependence on the asymmetry parameter of the energy levels of the nucleus in the "pure quadrupole case".

facing page 14.

These calculations have been carried through to the fourth order in η by Bersohn (B1). For all practical purposes an iteration procedure gives also an expansion in power of η^2 which converges rapidly for small value of η . This of course requires the explicit expression of the secular equation of degree $I + \frac{1}{2}$ from equation (14). Many cases of interest have been investigated namely: $I = 3/2$, $5/2$ (K1), $I = 7/2$ (D7) and $I = 9/2$ (C2). Cohen obtains his approximations using a method of continued fractions.

As an example we have plotted in fig. 1 the energy eigenvalue $E_i = \lambda_i e Q_{133}$ ($i = 1, 2, 3$) as a function of η for the special case $I = 5/2$ and compared the values obtained by exact solution of the secular determinant with those obtained by iteration expansion up to the fourth order in η . The secular equation is:

$$\lambda^3 - \frac{21}{400} (1 + \frac{1}{3} \eta^2) \lambda - \frac{1}{400} (1 - \eta^2) = 0 \quad (15)$$

while the expansions are:

$$\begin{aligned} \lambda_1 &= \frac{1}{4} (1 + 0.055 \eta^2 + 0.029 \eta^4) \\ \lambda_2 &= -\frac{1}{20} (1 - 1.500 \eta^2 + 0.958 \eta^4) \\ \lambda_3 &= -\frac{1}{5} (1 + 0.444 \eta^2 + 0.235 \eta^4) \end{aligned} \quad (16)$$

We can see that the expansions are reasonably accurate for $\eta < 0.7$. The use of higher terms in η will not improve the situation for $\eta > 0.7$ (except for the highest eigenvalue) because addition of terms will result in an oscillation around the true value.

No simple algebraic formula for transition frequency has been obtained. In practice the transition frequencies are more easily obtained by calculating the energy levels either by exact solution of the determinant equation (14), or by iteration method or else by perturbation theory (B1) (the $f(I, m_3)$ have been tabulated for half integral values of the spin by Bersohn in his thesis - or can be easily computed) and then by taking their differences divided by h . Transitions take place between adjacent levels only, when η is small, though other transitions have a small but not negligible transition probability as soon as $\eta \neq 0$. When $\eta \sim 1$, information about transition probabilities can be obtained by exact solution of the secular determinant, equation (14), which gives compatible simultaneous equations for the eigenfunctions. The knowledge of the unitary matrix that diagonalizes F_A enables one to find the matrix elements of the perturbing operator of which the squares are proportional to the transitions probabilities. The procedure is explained in some details in Cohen's thesis^(c2), and will not be repeated here since it gives no simple way of finding the direction of the principal axes contrary to the situation when the field is axially symmetric.

II. SPECTRA DUE TO COMBINED QUADRUPOLE AND ZEEMAN INTERACTIONS

When a nucleus with spin I is placed in a constant magnetic field \vec{H}_0 in the absence of all other interactions the Hamiltonian has the simple form:

$$\mathcal{H}_n = -g\beta \vec{H}_0 \cdot \vec{I} \quad (17)$$

Where \vec{I} is the angular momentum operator in the $1m_j$ representation.

A. Pure Zeeman Effect

When nuclei with spin I and zero quadrupole moment located in a crystal are subjected to a constant external magnetic field \vec{H}_0 , the net effect is the appearance for each nucleus of definite equidistant energy levels, if we neglect all kinds of dipole-dipole interactions mentioned in the Introduction. The single frequency of transition observed is $\nu = \frac{\mu H_0}{h I}$ and it is formed by the superposition of the $2I$ allowed transitions between the $2I+1$ Zeeman levels of each nucleus.

B. Small Zeeman Perturbation on the Quadrupole Spectra

We want to consider here the effect of this external magnetic field \vec{H}_0 when it is imposed on a crystal in which we have the quadrupole interaction discussed in the previous section and to study what happens when \vec{H}_0 assumes larger and larger constant values. When \vec{H}_0 is small, the energy due to Zeeman effect is small compared with the energy of the quadrupole coupling. As \vec{H}_0 increases, the energy of the two interactions becomes comparable and finally, for still larger value of \vec{H}_0 ,

the Zeeman energy is greater than the quadrupole energy. In this way the problem naturally splits into three regions of investigation. At both extremes we have the situation where either effect can be considered as a perturbation on the other, and in between, the region where both effects are equally important. We will first treat the case of a crystal placed in a weak magnetic field perturbing the quadrupole spectra.

To compare energies we use the following useful ratio: The magnetic energy given by equation (17) has its maximum absolute value when the spin is almost aligned with the magnetic field, ie. when the magnetic quantum number $m_j = I$. The quadrupole energy also has its maximum energy when $m_j = I$. So for the ratio of magnetic to electric quadrupole energy we shall use:

$$R = \left| \frac{m_j g \beta H}{\frac{e Q \phi_{zz}}{4I(2I-1)} [3m_j^2 - I(I+1)]} \right|_{m_j=I} = \frac{g \mu H}{e Q \phi_{zz}}$$

Here again we introduce the useful division between axially symmetric and non symmetric field gradient cases. In case of an axially symmetric field gradient ($\eta = 0$) the Hamiltonian is

$$\mathcal{H}_s = \frac{e Q \phi_{zz}}{4I(2I-1)} [3\vec{I}_z^2 - \vec{I}^2] - g \beta \vec{H}_0 \cdot \vec{I} \quad (18)$$

If the external magnetic field \vec{H}_0 coincides with the direction of symmetry axis, the problem can be solved exactly for any value of \vec{H}_0 , since \mathcal{H}_s is diagonal and the energy levels are simply:

$$E_{m_j} = \frac{e Q \phi_{zz}}{4I(2I-1)} [3m_j^2 - I(I+1)] - g \beta H_0 m_j \quad (19)$$

All other cases appear as more or less important deviations from this very simple case. For this reason we will discuss it to some extent.

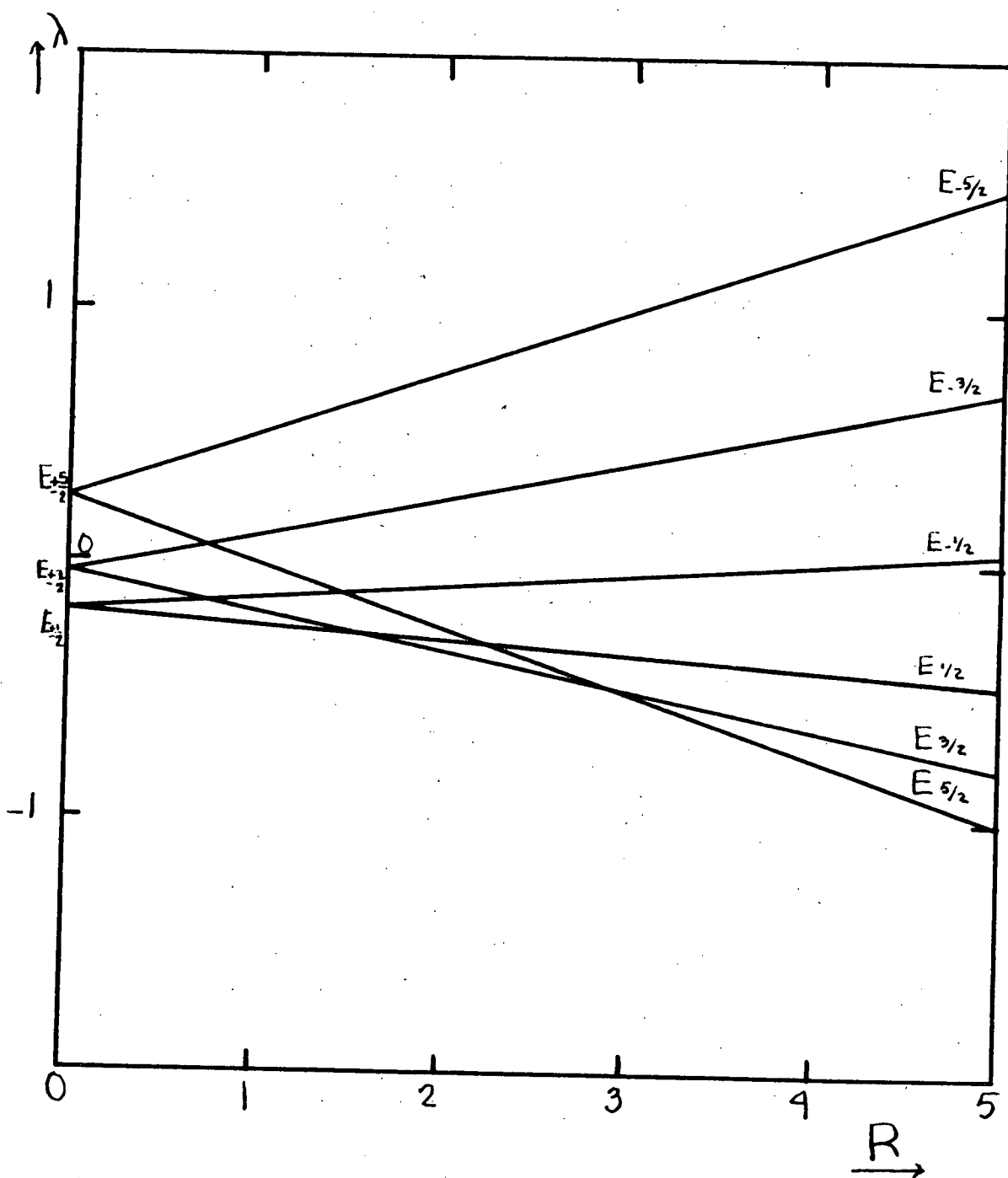


Figure 2. Energy levels for the case $I=5/2$, $\gamma = 0$ and the magnetic field in the direction of the z-axis, as a function of H .

facing page 18.

The introduction of the magnetic field has split the previous doubly degenerate quadrupole energy levels into two non degenerate ones equally spaced from the original by $\pm |m_3| g \beta H_0$. We have sketched roughly in fig. 2 the energy spectrum as a function of \vec{H}_0 for the case of $I = 5/2$. For large values of \vec{H}_0 we obtain the Zeeman spectrum perturbed by comparatively small quadrupole interaction.

There are $2I$ allowed transitions between the $2I+1$ levels, since each energy eigenvalue belongs to only one eigenfunction ψ_{m_3} of the $I m_3$ representation. These frequencies are given by:

$$\nu_{|m_3| \rightarrow |m_3|-1} = \left| \frac{e Q \beta_2}{4I(2I-1)} 3(2|m_3|-1) \mp g \beta H_0 \right|, \quad m_3 \geq \frac{1}{2}$$

with + sign if $m_3 = -|m_3|$
and - sign if $m_3 = +|m_3|$ (20)

and

$$\nu_{+\frac{1}{2} \rightarrow -\frac{1}{2}} = |g \beta H_0| = \nu_0(H_0)$$

When \vec{H}_0 or R is large, and when we are well in the region in which the Zeeman energy is large compared to quadrupole energy, the spectra for half integral I can be described in terms of the central component ν_0 (P_0, V_2, V_3, P_2) which is surrounded by $(2I-1)$ satellites appearing symmetrically in pairs on each side of it.

If the \vec{H}_0 magnetic field \vec{H}_0 is perpendicular to \vec{H}_b as is usually the case, the relative intensity of each line is proportional to:

$$\frac{1}{4} H_0^2 [I(I+1) - m_3(m_3-1)] \quad (21)$$

and so for the region of large magnetic field H_0 the central component $\nu_0(H_0)$ is the most intense with the first, second,

etc., satellites on each side appearing with decreasing intensities.

As soon as we depart from this very special case, the problems become much more involved. If $\eta=0$ but the constant external magnetic field H_0 is no more parallel to the z axis of the crystal we already have complications. Assume that the magnetic field lies in the x - z plane (where the x axis is arbitrary) and let the angle between the direction of H_0 and the z axis be θ .

Then from equation (18) we have for the Hamiltonian:

$$\mathcal{H}_s = \frac{eQ\varphi_{zz}}{4I(2I-1)} [3\vec{I}_z^2 - \vec{I}^2] - g\beta H_0 (\vec{I}_x \sin\theta + \vec{I}_z \cos\theta) \quad (22)$$

with the matrix elements given in equation (5) supplemented by the new elements:

$$(m_3 | \mathcal{H}_s | m_3) = -g\beta H_0 m_3 \cos\theta \quad (23)$$

$$(m_3 | \mathcal{H}_s | m_3 \pm 1) = -\frac{g\beta H_0}{2} \sqrt{I(I+1) - m_3(m_3 \pm 1)} \sin\theta$$

The energy levels are obtained exactly by solving the secular determinant of \mathcal{H}_s for E which is of the form: $|\mathcal{H}_s m_3 m_3' - E \delta_{m_3 m_3'}| = 0$

But if $R \ll 1$ a perturbation calculation (degenerate case) can be performed in which the quadrupole part is considered as the unperturbed Hamiltonian and the magnetic as the perturbation. The expression for the energy levels are given by Kruger (K1) who also discusses the spectra to be obtained. He shows that we have for certain orientation of the crystal a non negligible transition probability between levels other than adjacent - which at first glance seems to violate the selection rules for magnetic dipole transitions. Expansions of this type hold as long as the energy levels have not already started crossing each other.

The next and last complication comes in when we consider that the electric field gradient is not axially symmetric ($\eta \neq 0$). The Hamiltonian in this case is given by equation (18) to which we add the asymmetric part of the quadrupole interaction:

$$\mathcal{H}_A = \mathcal{H}_S + \frac{eQq_{zz}}{4I(2I-1)} (\vec{I}_x^2 - \vec{I}_y^2) \eta \quad (24)$$

The problem can be solved exactly with the resulting secular determinant. But again if \vec{H}_0 is small the energy levels can be obtained by an expansion in powers of \vec{H}_0 around the unperturbed energy levels which are in this case the quadrupole levels that can be found in case of axial asymmetry by the methods discussed in the previous section, either approximately or exactly. This procedure is carried out completely to the third order by Bersohn (B1). His expansion requires that \vec{H}_0 , η and θ (the angle between \vec{H}_0 and the z axis) be small. Perturbation theory along this line is cumbersome and does not in general lead to formulae of great applicability.

C. Small Quadrupole Perturbation on the Zeeman Effect

When the Zeeman energy is large compared to the quadrupole energy, ie. when $\mu H_0 \gg \frac{eQq_{zz}}{4}$, then the quadrupole effect can be considered as a perturbation on the Zeeman pattern (section II A). This perturbation theory has been extensively treated by various authors. The spectrum is usually described in terms of the central component ν_0 , which appears when I is half integral, and which can be shifted, and pairs of satellites, whose distances from the central components are functions of the

orientation of the crystal with respect to the constant magnetic field \vec{H}_0 . By rotation of the crystal in the field \vec{H}_0 , the orientation of the principal axes can be recognized. Explicit expressions for this perturbation can be found in the literature for axially symmetric (P6) as well as for the asymmetric (V2, V3) cases.

III. EQUALLY STRONG QUADRUPOLE AND ZEEMAN INTERACTIONS

We are now left with the problem of a double interaction where the electric quadrupole interaction is comparable with the Zeeman energy. This problem requires the complete solution of the secular determinant, since as we have seen in the previous section both perturbation theories break down in that region. In this section we will proceed to set up this secular equation in the case $I = 5/2$ and to give the solution for two particularly simple cases. We have used in the discussion that follows the data obtained in Dr. Volkoff's laboratory for the case of Al^{27} in a spodumene crystal and have stated our result in a form that will fit directly a proposed experiment.

A. Secular determinant for the case $I = 5/2$.

We have set up in eq. (24) the Hamiltonian for a nucleus with spin I , magnetic moment $\vec{\mu}$, quadrupole moment eQ , placed in a crystal with non axially symmetric field gradient submitted to a constant external magnetic field H making with the z -axis an angle θ in the x - z plane. It should be emphasized at this point that the particularly simple form of eq. (24) results from the fact that the xyz axes have been chosen to coincide with the principal axes of the field gradient tensor, which accounts for the absence of cross terms of the form $\hat{I}_x \hat{I}_y$, etc. We also know what the non-zero matrix elements are from equations (19) and (23). Examination of the problem reveals that we have to deal with 4 parameters: I, η, θ, R . Moreover the secular equation to be solved is of degree $2I+1$ in general, which means for our particular choice of I , the 6th degree; hence there is no hope of

obtaining a general analytic solution.

We want to find the solution of the time-independent Schrodinger equation:

$$\mathcal{H}_A \chi_i = E_i \chi_i \quad (i = 1, 2, 3, 4, 5, 6) \quad (25)$$

where χ_i is a linear combination of the eigenfunctions of the I, m_z , representation. Let the latter be $\psi_{\frac{5}{2}}, \psi_{\frac{3}{2}}, \psi_{\frac{1}{2}}, \psi_{\frac{1}{2}}, \psi_{\frac{3}{2}}, \psi_{\frac{5}{2}}$; then:

$$\chi_i = \sum_m a_{im} \psi_m \quad (26)$$

Eq. (25) can be thought of as a matrix equation where \mathcal{H}_A is a 6X6 matrix and χ_i a column matrix of the form

$$\begin{bmatrix} a_{i,5/2} \\ a_{i,3/2} \\ a_{i,1/2} \\ a_{i,-1/2} \\ a_{i,-3/2} \\ a_{i,-5/2} \end{bmatrix}$$

the equality sign in eq. (25) will hold for certain values of E_i only, those values which make the system of simultaneous equations compatible; ie., the E_i which make the determinant of the coefficients vanish. In matrix language this also means that we find the new representation in which \mathcal{H}_A is diagonal; the unitary transformation by which this is to be effected, S , will be given by the coefficients $a_{i,m}$.

For $I = 5/2$, the secular determinant is:

$$\begin{vmatrix} a & g & h & 0 & 0 & 0 \\ g & b & i & j & 0 & 0 \\ h & i & c & k & j & 0 \\ 0 & j & k & d & i & h \\ 0 & 0 & j & i & e & g \\ 0 & 0 & 0 & h & g & f \end{vmatrix} = 0 \quad (27)$$

$$\text{where } a = -E_i - B \cos \theta + \frac{A}{4}$$

$$d = -E_i + \frac{B \cos \theta}{5} - \frac{A}{5}$$

$$b = -E_i - \frac{3B \cos \theta}{5} - \frac{A}{20}$$

$$e = -E_i + \frac{3B \cos \theta}{5} - \frac{A}{20}$$

$$c = -E_i - \frac{B \cos \theta}{5} - \frac{A}{5}$$

$$f = -E_i + B \cos \theta + \frac{A}{4}$$

$$g = -\frac{B \sin \theta}{\sqrt{5}}$$

$$j = \frac{3A\hbar}{20\sqrt{2}}$$

$$h = \frac{A\hbar}{4\sqrt{10}}$$

$$k = -\frac{3B \sin \theta}{5}$$

$$i = -\frac{\sqrt{8} B \sin \theta}{5}$$

$$\text{and } B = \mu H$$

$$A = e\hbar^2 \gamma_z$$

The 73 terms of the expansion reduce to the following 6th degree equation:

$$\sum_{s=0}^6 c_s E_i^s = 0$$

$$\text{where } c_6 = 1$$

$$c_5 = 0$$

$$c_4 = -\frac{7B^2}{5} - \frac{21A^2}{200} - \frac{7A^2}{200} \hbar^2$$

$$c_3 = -\frac{A^3}{200} + \frac{28AB^2 \hbar^2}{125} - \frac{56AB^2 \hbar^2}{125} - \frac{28AB \hbar^2}{125} \hbar^2 + \frac{A^3}{200} \hbar^2$$

$$c_2 = \frac{259B^4}{625} - \frac{6A^2B^2p^2}{125} + \frac{123A^2B^2q^2}{2500} + \frac{441A^4}{160000} - \frac{81A^2B^2q^2}{1250} \eta +$$

$$+ \left(\frac{17A^2B^2p^2}{625} - \frac{13A^2B^2q^2}{2500} + \frac{147A^4}{80000} \right) \eta^2 + \frac{49A^4}{160000} \eta^4$$

$$c_1 = -\frac{3B^5p^3q^2}{625} + \frac{88AB^4p^4}{625} - \frac{44AB^4q^4}{625} + \frac{106AB^4p^2q^2}{625} + \frac{3A^2B^3pq^2}{625} -$$

$$- \frac{7A^3B^2p^2}{1000} - \frac{17A^3B^2q^2}{5000} + \frac{21A^5}{8000} + \left(\frac{44AB^4q^2}{625} - \frac{3A^3B^2q^2}{2500} \right) \eta +$$

$$+ \left(\frac{19A^3B^2p^2}{5000} + \frac{A^3B^2q^2}{200} - \frac{7A^5}{40000} \right) \eta^2 - \frac{A^3B^2q^2}{2500} \eta^3 -$$

$$- \frac{7A^5}{80000} \eta^4$$

$$c_0 = -\frac{9B^6p^6}{625} - \frac{9B^6q^6}{625} - \frac{24B^6p^4q^2}{625} - \frac{27B^6p^2q^4}{625} + \frac{3AB^5p^3q^2}{2500} +$$

$$+ \frac{77A^2B^4p^4}{5000} + \frac{A^2B^4p^2q^2}{1250} - \frac{A^2B^4q^4}{5000} - \frac{161A^4B^2p^2}{160000} - \frac{41A^2B^2q^2}{160000} +$$

$$+ \frac{A^6}{160000} - \left(\frac{A^2B^4p^2q^2}{1250} + \frac{13A^2B^4q^4}{1250} + \frac{A^4B^2q^2}{4000} \right) \eta +$$

$$+ \left(-\frac{9A^2B^4p^4}{5000} + \frac{13A^4B^2p^2}{80000} - \frac{47A^4B^2q^2}{80000} + \frac{17A^2B^4q^4}{5000} - \frac{A^6}{80000} \right) \eta^2 +$$

$$+ \frac{A^4B^2q^2}{4000} \eta^3 - \left(\frac{9A^4B^2}{160000} - \frac{A^6}{160000} \right) \eta^4$$

$$\text{and where } p \equiv \cos \theta \quad \text{and } q \equiv \sin \theta \quad (28)$$

The six eigenvalues of the problem are the roots of this equation.

Once they are known, the $a_{i,m}$'s can be found with any five of the six simultaneous equations (25) and their values

in terms of any one of the a 's with an additional condition of normalization:

$$\sum_m (a_{im}^* a_{im}) = \sum_m a_{im}^2 = 1 \quad (29)$$

The determinant has a particularly simple form in the case of $\theta = 0^\circ$, since the Zeeman energy is then diagonal in the representation chosen. We will see later that it is possible to apply a transformation and to obtain a determinant of the same form in case where the field \vec{H} is in the direction of the two other principal axes (section III C). Two parameters R and γ are then left that are to be fixed later.

B. Case of $\theta = 0^\circ$

The determinant (27) has the form:

$$\begin{vmatrix} a' & 0 & h' & 0 & 0 & 0 \\ 0' & b' & 0 & j' & 0 & 0 \\ h' & 0 & c' & 0 & j' & 0 \\ 0 & j' & 0 & d' & 0 & h' \\ 0 & 0 & j' & 0 & e' & 0 \\ 0 & 0 & 0 & h' & 0 & f' \end{vmatrix} = 0 \quad (30)$$

with: $a' = -\lambda_i - \Gamma + \frac{1}{4}$

$d' = -\lambda_i + \frac{\Gamma}{5} - \frac{1}{5}$

$b' = -\lambda_i - \frac{3\Gamma}{5} - \frac{1}{20}$

$e' = -\lambda_i + \frac{3}{5}\Gamma - \frac{1}{20}$

$c' = -\lambda_i - \frac{\Gamma}{5} - \frac{1}{5}$

$f' = -\lambda_i + \Gamma + \frac{1}{4}$

$h' = \frac{\gamma}{4\sqrt{10}}$

$j' = \frac{3\gamma}{20\sqrt{2}}$

$\lambda_i = \frac{E_i}{A} \quad \Gamma = \frac{B}{A} = \frac{R}{4}$

By interchange of columns (the 3rd, one to the left and the 5th, two to the left) and of rows (the 3rd, one up and the 5th, two up) det (30) now looks:

$$\begin{vmatrix} a' & h' & 0 & 0 & 0 & 0 \\ h' & c' & j' & 0 & 0 & 0 \\ 0 & j' & e' & 0 & 0 & 0 \\ 0 & 0 & 0 & b' & j' & 0 \\ 0 & 0 & 0 & j' & d' & h' \\ 0 & 0 & 0 & 0 & h' & f' \end{vmatrix} = 0 \quad (31)$$

or in block determinant:

$$\begin{vmatrix} L & 0 \\ 0 & M \end{vmatrix} = 0 \quad (32)$$

So the problem is reduced in this case to the solution of two 3X3 determinants giving us the required six roots of (31). If now we expand the two determinants we have two independent cubic equations to be solved:

$$\begin{aligned} \text{From L : } -\lambda'^3 - \frac{3}{5} \Gamma \lambda'^2 + \left(\frac{13}{25} \Gamma^2 - \frac{6}{25} \Gamma + j'^2 + h'^2 + \frac{21}{400} \right) \lambda' + \\ + \left[\frac{3}{25} \Gamma^3 + \frac{2}{25} \Gamma^2 - \left(\frac{3}{80} - j'^2 + \frac{3}{5} h'^2 \right) \Gamma + \frac{1}{400} - \frac{1}{4} j'^2 + \frac{h'^2}{20} \right] = 0 \end{aligned} \quad (33)$$

$$\begin{aligned} \text{and from M : } -\lambda''^3 + \frac{3}{5} \Gamma \lambda''^2 + \left(\frac{13}{25} \Gamma^2 + \frac{6}{25} \Gamma + j''^2 + h''^2 + \frac{21}{400} \right) \lambda'' - \\ - \left[\frac{3}{25} \Gamma^3 - \frac{2}{25} \Gamma^2 - \left(\frac{3}{80} - j''^2 + \frac{3}{5} h''^2 \right) \Gamma - \frac{1}{400} + \frac{1}{4} j''^2 - \frac{h''^2}{20} \right] = 0 \end{aligned} \quad (34)$$

The supercripts are being placed to indicate in the following discussion from which determinant the roots come from, since as we will then see each set of three roots belongs to a particular set of eigenfunctions.

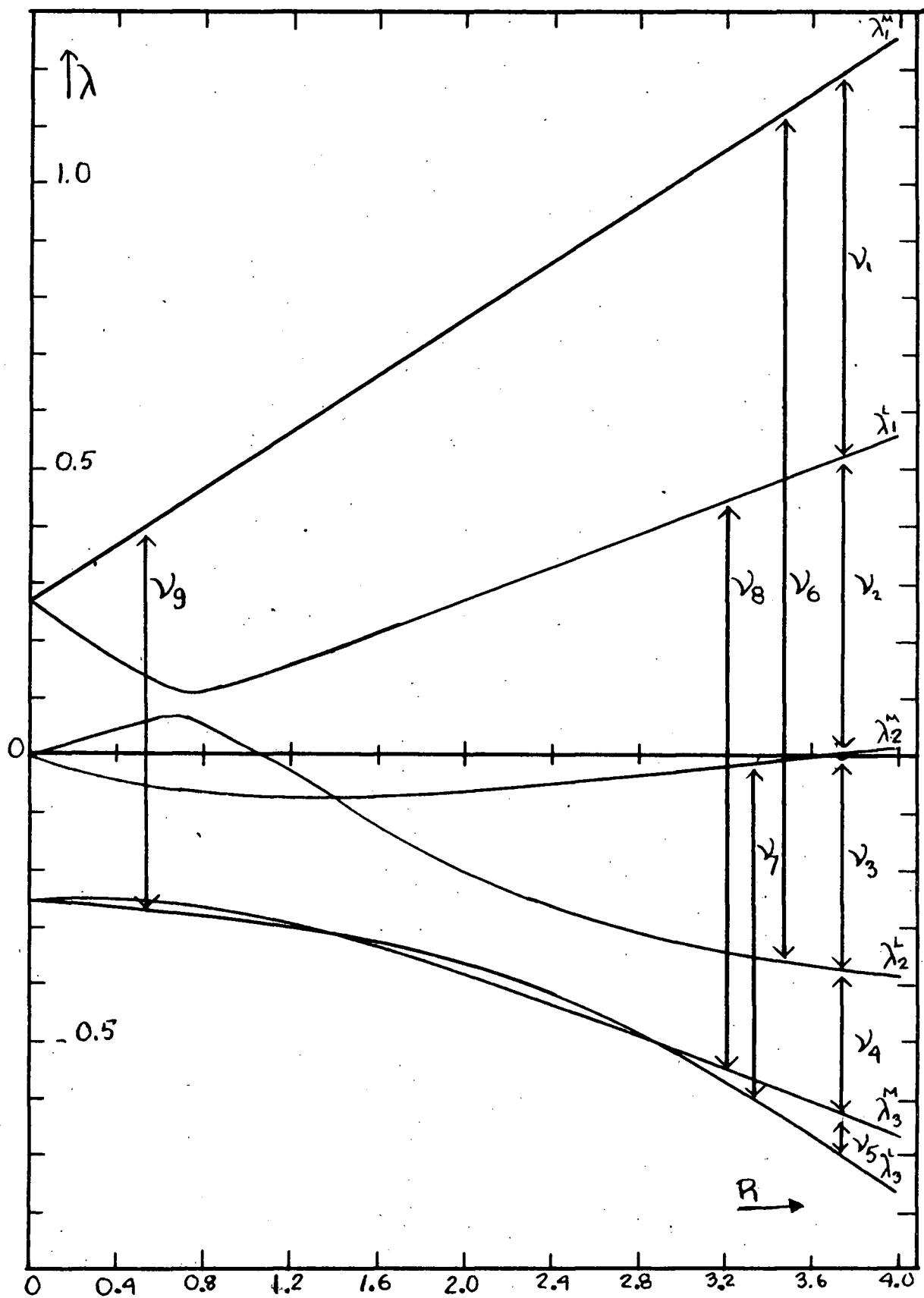


Figure 3. Energy levels for the special case, $I = 5/2$, $\eta = 0.95$ and $\theta = 0^\circ$, as a function of R . facing page 28.

Equations (33) and (34) can now be solved exactly for λ as a function of Γ for a particular value of η or as a function of η for a particular value of Γ . The λ being eigenfunctions of a physical problem are real, and so the cubic equations have to be solved by trigonometric method, but the analytic expressions obtained do not furnish algebraic expressions that can be handled easily.

As we have already stated we proceed to solve the problem with numerical values of immediate interest in an actual experimental case. We refer to the case of Al^{27} in spodumene crystal, for which the orientation of the principal axes xyz of the field gradient tensor, the axial asymmetry parameter $\eta = 0.95$, the magnetic moment $\vec{\mu}$ and the quadrupole constant $\frac{eQq_{23}}{4} = \frac{18}{4R} = 2.960 \text{ Mc/sec}$ are known. Using these data we investigate the behavior of the eigenvalues, transition frequencies and probabilities as a function of the external magnetic field \vec{H} which can assume any constant value from 0 upwards, thus covering the complete range of energy ratio R . The r.f. field \vec{H}_1 , used to detect the transition lines is assumed to be at 90° from \vec{H} .

Having inserted $\eta = 0.95$ in equations (33) and (34) we have solved numerically these equations for λ as a function of $\Gamma = \frac{R}{4}$. The eigenvalues are plotted in figure 3 for $0 \leq R \leq 4$.

The three regions mentioned in section II are $0 \leq R \ll 1$, where the perturbation theory of a small Zeeman perturbation on a large quadrupole effect holds; $R \sim 1$ where no perturbation theory can be applied successfully, and $R \gg 1$ where the perturbation theory of the Zeeman levels by small quadrupole interaction applies successfully.

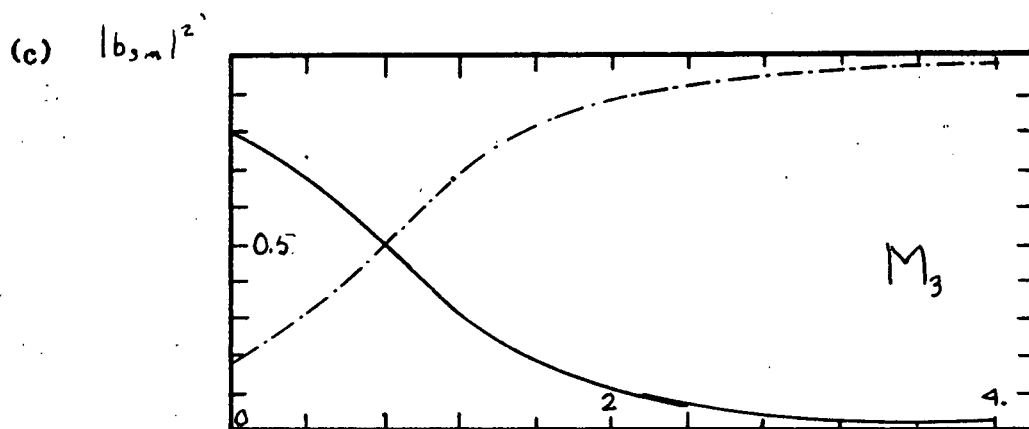
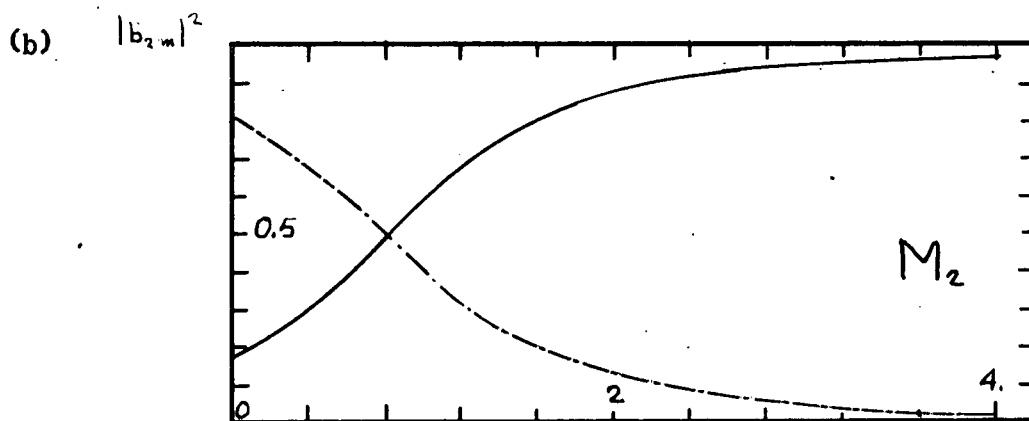
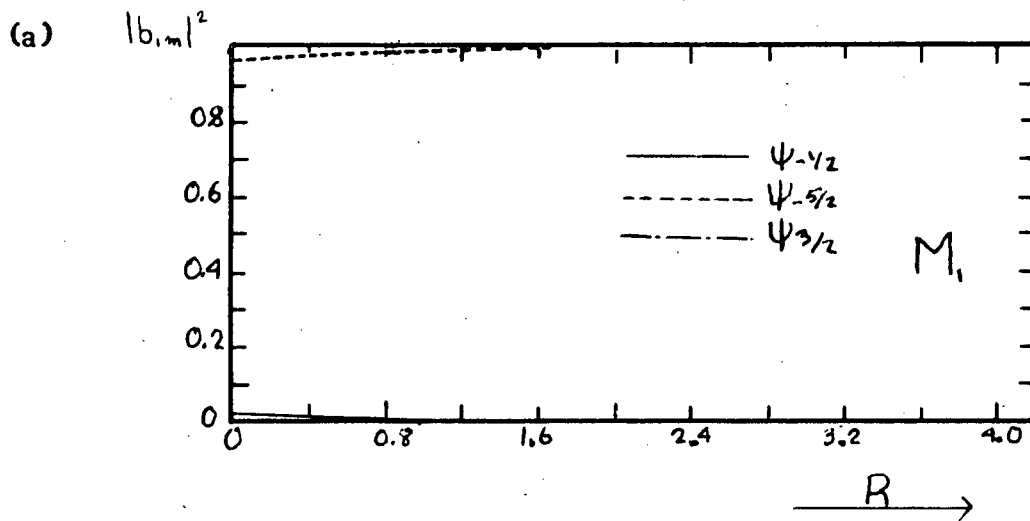


Figure 5. Square of the coefficients of the eigenfunctions for the eigenvalues of fig. 3, as a function of R
 Group M . facing page 29.

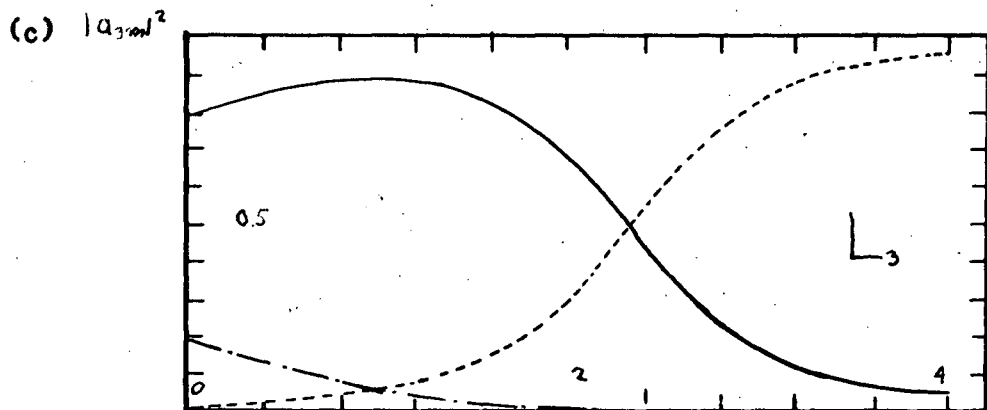
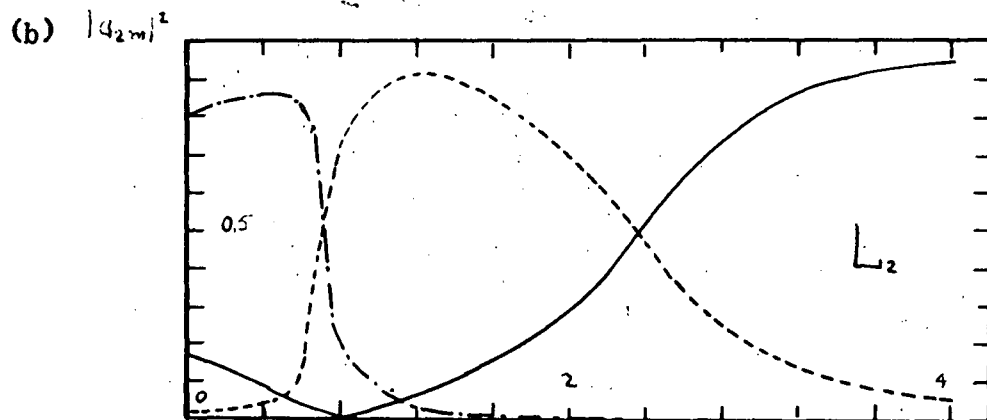
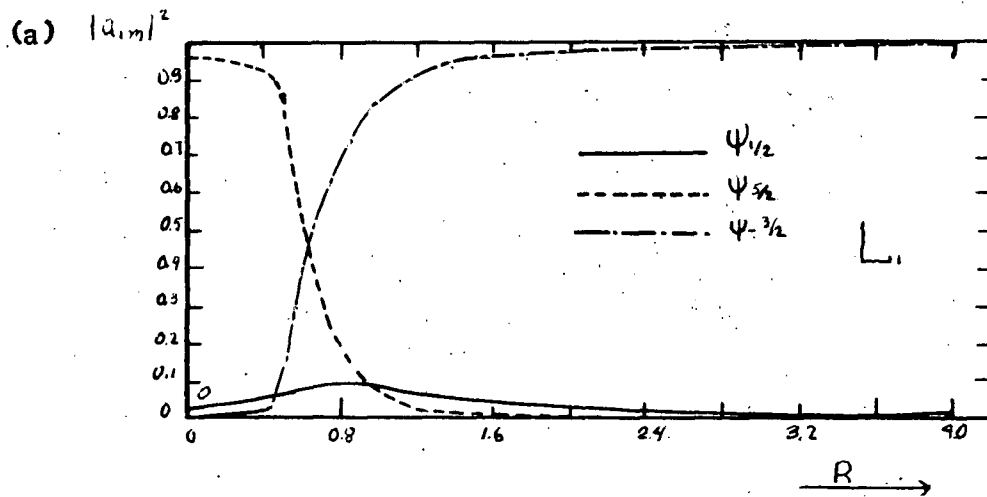


Figure 4. Square of the coefficients of the eigenfunctions for the eigenvalues of fig. 3, as a function of R Group L .

facing page 29.

It can be seen at once that the behavior of the eigenvalues is different from that we have sketched in fig. 2 for the simplest possible case of double interactions. The eigenvalues do not all cross each other, but some of them do, while others just come near and repel each other as R increases. A clear understanding of this behavior will be available when the eigenfunctions will be found.

By considering how equations (33) and (34) were arrived at, ie., how the det (31) was obtained it should be clear that the λ_i^L belong to a linear combination of $\psi_{\frac{3}{2}}, \psi_{\frac{1}{2}}$ and $\psi_{\frac{5}{2}}$ while the λ_i^M belong to a linear combination of $\psi_{-\frac{3}{2}}, \psi_{-\frac{1}{2}}$ and $\psi_{\frac{3}{2}}$. The coefficients of the eigenfunctions belonging to the λ_i^L are found through equation (25):

$$\begin{aligned} a_{i, \frac{1}{2}} &= \frac{(\lambda_i + \Gamma - \frac{1}{4})}{h'} a_{i, \frac{5}{2}} \\ a_{i, -\frac{3}{2}} &= \frac{\lambda'}{(\lambda_i - \frac{3}{2}\Gamma + \frac{1}{20})} a_{i, \frac{1}{2}} \\ a_{i, \frac{3}{2}}^2 + a_{i, \frac{1}{2}}^2 + a_{i, -\frac{3}{2}}^2 &= 1 \end{aligned} \tag{35}$$

A similar expression can be derived for the eigenfunctions belonging to the λ_i^M . The corresponding coefficients are denoted by b 's in fig. 5.

Now, the squares of the $a_{i,m}$'s will give the probability for the nucleus to be found in the state ψ_m when its eigenvalue is λ_i . We have plotted in fig. 4 and 5 these probabilities for all λ_i as a function of R between 0 and 4.

In the case of pure quadrupole interaction ($R=0$) with $\eta \neq 0$ the degenerate state with the highest eigenvalue consists almost entirely of $\psi_{\frac{3}{2}}$ and $\psi_{-\frac{3}{2}}$, while the probability of finding the nucleus in the states $\psi_{\frac{3}{2}}, \psi_{-\frac{3}{2}}, \psi_{-\frac{1}{2}}$ and $\psi_{\frac{1}{2}}$ is less

altogether than 5%. The state of intermediate energy consists mostly of $\psi_{\frac{3}{2}}$ and $\psi_{-\frac{3}{2}}$, and the chance of finding the nucleus in the states $\psi_{\frac{1}{2}}$ and $\psi_{-\frac{1}{2}}$ and 1% in $\psi_{\frac{5}{2}}$ and $\psi_{-\frac{5}{2}}$ is about 18%. Finally the state of lowest energy consists mostly of $\psi_{\frac{1}{2}}$ and $\psi_{-\frac{1}{2}}$, but again there is a contribution of 18% from $\psi_{\frac{3}{2}}$ and $\psi_{-\frac{3}{2}}$, and 1% from $\psi_{\frac{5}{2}}$ and $\psi_{-\frac{5}{2}}$. So we now can expect a non-zero transition probability from the highest to the lowest levels, which was completely forbidden in the case of axial symmetry. In this latter case the highest eigenvalue would belong entirely to $\psi_{\frac{5}{2}}$ and $\psi_{-\frac{5}{2}}$, the middle to $\psi_{\frac{3}{2}}$ and $\psi_{-\frac{3}{2}}$, and the lowest to $\psi_{\frac{1}{2}}$ and $\psi_{-\frac{1}{2}}$; so that transitions between the highest and the lowest levels would be strictly forbidden by the selection rule for magnetic dipole transitions. In this case also the introduction of a magnetic field \vec{H} along the z-axis would split the degenerate levels as indicated on figure 2, resulting in the crossing of the eigenvalues.

In the present case, however, the situation is quite different. The states are divided into two classes (or "races" to employ the term that Heitler for instance uses in a similar situation)(10). The class L consist of a linear combination of $\psi_{-\frac{3}{2}}$, $\psi_{\frac{1}{2}}$ and $\psi_{\frac{5}{2}}$, while the class M consist of a linear combination of $\psi_{-\frac{5}{2}}$, $\psi_{-\frac{1}{2}}$ and $\psi_{\frac{3}{2}}$. Levels belonging to different classes may cross each other, but levels of the same class will "repel" each other. Let us study closely the states of class L, as a function of R. If we consider graph (a) in fig. 4, we can see that the state L_1 up to $R = 0.4$ consists mostly of $\psi_{\frac{5}{2}}$. Then as R increases it becomes mostly characterized by $\psi_{-\frac{3}{2}}$, the more so as R further increases. So we would be justified to label this eigenvalue $m_j = -\frac{3}{2}$.

for sufficiently large values of R as this is how we usually label it in the pure Zeeman effect; in other words, if it were not for the axially asymmetric quadrupole interaction this eigenvalue would belong uniquely to $\psi_{-\frac{3}{2}}$.

A consideration of the state L_2 now will explain what exchange of character has taken place and how the phenomenon of "repulsion of levels of the same class" can be explained in terms of the eigenfunctions. L_2 is mostly characterized by $\psi_{-\frac{3}{2}}$ up to $R \sim 0.4$. Then as R increases its eigenfunction shows a large amount of $\psi_{\frac{5}{2}}$. L_1 and L_2 have exchanged their respective roles. But eventually L_2 would become a $m_z = \frac{1}{2}$ Zeeman level, and it is clear that it must again exchange role this time with L_3 . This we can see again by looking at the graphs in fig. 4.

The states of class M consist of linear combinations of the $\psi_{\frac{5}{2}}$, $\psi_{-\frac{1}{2}}$ and $\psi_{\frac{3}{2}}$; a similar analysis of their behavior can be made with the help of the three graphs of fig. 5. The eigenvalues of class M will cross those of class L, since there is then no possibility of an exchange of characters, whereas among themselves they will only come near each other and repel each other as R increases. M_1 , consisting mostly when $R=0$, of $\psi_{-\frac{5}{2}}$ is already in its proper position for the Zeeman effect and its characteristics simply become stronger and stronger as R increases.

TRANSITION FREQUENCIES: The selection rule for magnetic dipole transitions $|m - m'| = 1$ indicates at once that transitions are to be expected only between levels belonging to different classes, but not between levels of the same class, i.e.,

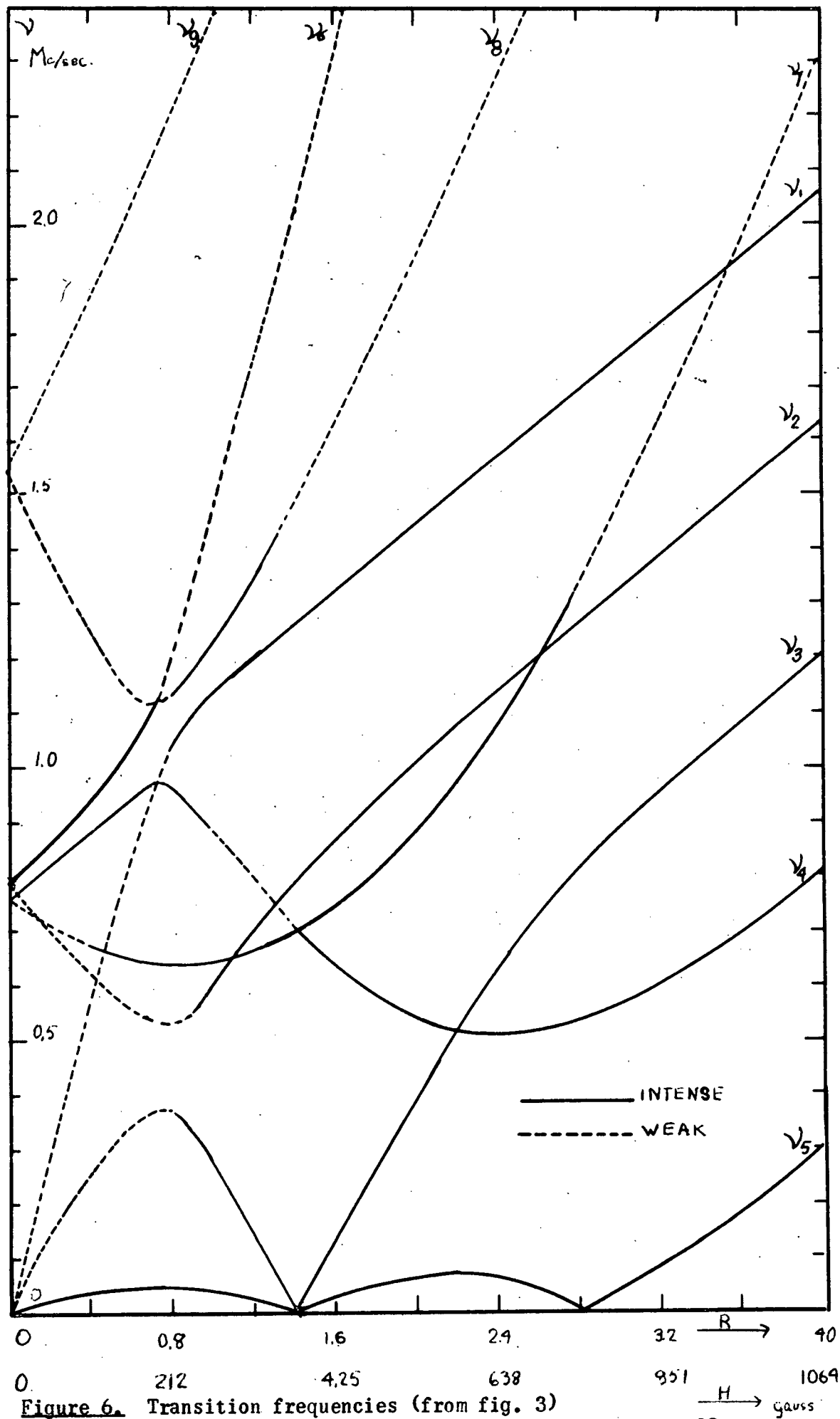


Figure 6. Transition frequencies (from fig. 3) as a function of R .

facing page 32.

only between the L and the M levels. There are 9 such possibilities as shown in fig. 3. Five of them, numbered from 1 to 5 are the expected Zeeman transitions, those lines that represent transitions between adjacent levels. The four other transitions are from this point of view "forbidden". Three of them, numbered from 6 to 8 are sums of three Zeeman lines and the last, 9, is obtained by adding together the 5 Zeeman lines.

We have plotted in figure 6 the frequencies of these 9 transitions as functions of R. The frequencies in Mc/sec have been fixed with the help of the value of the quadrupole constant for Al^{27} in spodumene (P2): 2.960 Mc/sec. The frequencies are given by $\nu_{ij} = |\lambda_i - \lambda_j| \frac{e Q p_{32}}{h}$

The central Zeeman component ν_3 (the one which in equation (20) was called ν_0) takes on its usual significance only when $R > 1.6$. For large magnetic fields it is the central line discussed in the literature on quadrupole perturbation on the Zeeman effect.

Of these 9 lines, some will be too weak to be observed, while others will escape detection because of their very low frequencies.

TRANSITION PROBABILITIES: The net number of transitions between two energy levels, L_i and M_j is proportional to the difference in population of the two levels and to the square of the absolute value of the ij -matrix element of the time dependent perturbation operator causing the transitions. The energy difference involved in the transitions between the various

orientations of the nuclei is very small compared to the energy of thermal agitation. The population of the levels is given by $N_i = N_0 e^{-\frac{E_i}{RT}}$ where N_0 is the population of the ground level and E_i is the energy difference between the given level and the ground level. Since $E_i \ll kT$ for all i , all levels are almost equally populated, their population being given in first approximation by $N_i = N_0 (1 - \frac{E_i}{kT})$. Hence the fractional difference in population between the j th. and the ground state is given by $|\frac{\Delta_j}{kT}|$ (of the order of 10^{-6} ^{at room temperature} if $\nu = 30$ Mc/sec. Thus the net number of transitions between two states will depend on the frequency of transition and on the square of the absolute value of the matrix element.

Since the relative intensity of the expected lines is thus seen to be determined to a large extent by the square of the absolute value of the matrix element we now proceed to calculate it and to plot it as a function of R for each of the I lines for which it does not vanish identically.

If the r-f magnetic field \vec{H}_1 is perpendicular to \vec{H}_0 , the perturbing operator is simply

$$\mathcal{H}_p' = H_1 [(\vec{I}_x + i\vec{I}_y) e^{-i\omega t} + (\vec{I}_x - i\vec{I}_y) e^{i\omega t}] \quad (36)$$

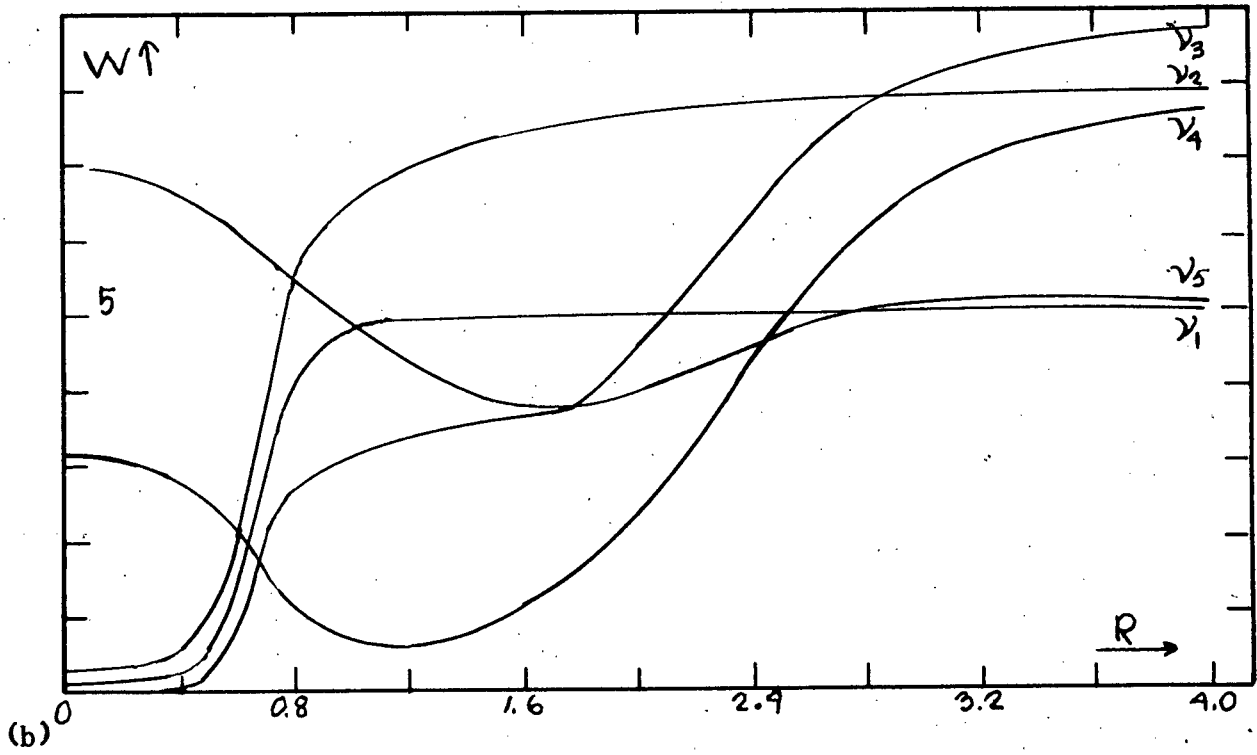
and the transition probabilities are given by:

$$W_{i \rightarrow j} \propto |(i | \mathcal{H}_p' | j)|^2 \quad (37)$$

where \mathcal{H}_p' is taken in the system of representation which diagonalizes \mathcal{H}_A . But we already know the unitary transformation S which diagonalizes \mathcal{H}_A now that we know exactly the $a_{i,m}'$'s. Hence:

$$\mathcal{H}_p' = S^{-1} \mathcal{H}_p S. \quad (38)$$

(a)



(b)

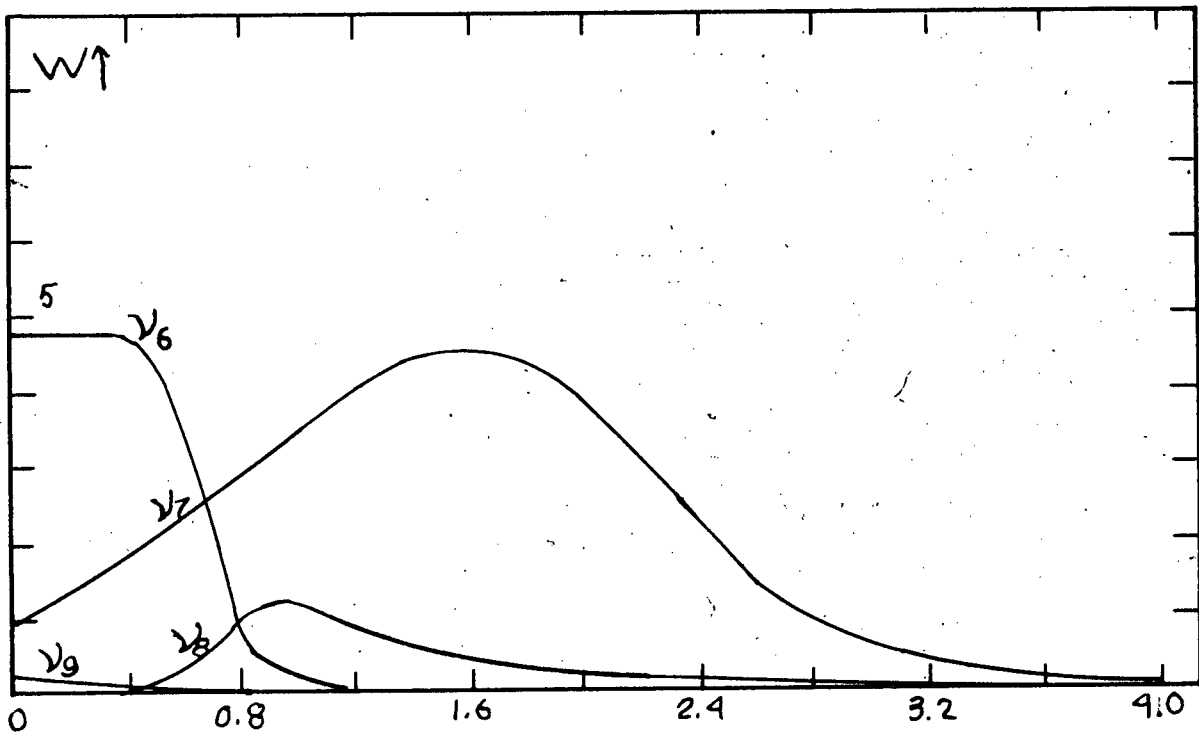


Figure 7. Square of the matrix elements of the perturbing operator \mathcal{H}'_p (in arbitrary units) as a function of R .

facing page 34.

And so:

$$W_{i \rightarrow j} \propto |(i | S^{-1} (\vec{I}_x + i \vec{I}_y) S | j)|^2 H^2 \quad (39)$$

We have plotted with an arbitrary ordinate the $W_{i \rightarrow j}$ in fig. 7 as a function of R between 0 and 4, for the 9 lines. They appear in two groups. In a) we have the five Zeeman lines, and in b) the four "forbidden lines".

Of the Zeeman lines, ν_1, ν_2 and ν_3 are very weak in the region of large quadrupole effect and their transition probability increases rapidly around $R=0.8$, ν_4 and ν_5 are expected to be observed for all values of R through ν_4 might be too weak in region $0.8 < R < 1.6$ and ν_5 of too low frequency for all $R < 4$. When $R > 2.8$, we have the same kind of spectrum as observed for the case of a large Zeeman energy perturbed by a small quadrupole effect, (P.6). The central component ν_3 usually denoted by ν has the greatest intensity, while the inner satellites are weaker but of equal intensity, and the outer satellites weaker still.

It is to be remarked that the so-called "forbidden lines" received their name from the fact they correspond to transitions between energy levels that are not adjacent. But the detailed analysis we have given above of the eigenfunctions should make it clear that they are as allowed as any other inasmuch as they contain a certain amount of ψ_m for one of them and $\psi_{m'}$ for the other, where $|m - m'| = 1$. For instance, inspection of graph c) fig. 4, and of graph b) fig. 5, will show that a transition is to be expected between levels λ_2^m and λ_3^l , since a transition between the eigenfunctions $\psi_{\frac{3}{2}}$ in M_2 and $\psi_{\frac{1}{2}}$ in L_3 , as well as a transition

between ψ_i in L_3 and ψ_z in M_2 are possible. In fact these transitions are responsible for the large intensity of the line ν_7 as shown by graph b) of figure 7 when $0 \leq R < 2.8$. Of the forbidden lines ν_6 might also be expected in the region of small R . It is one of the components of the allowed transitions for the pure quadrupole, the other being ν_2 . The forbidden transition of the pure quadrupole which is in fact formed by the superposition of ν_9 and ν_8 is very weak. Its components will not be detected when \vec{H} increases, except perhaps ν_8 around $R \sim 0.8$.

More precise information of the frequencies and the squares of the matrix elements will be obtained from Table I for R from 0 to 4, at intervals of 0.4. On the other hand we have tried to bring^{out} this information on the graph of fig. 6 by using plain lines for relatively intense transitions (> 1 in a.u. unit) and dashed ones otherwise.

COMPARISON WITH PERTURBATION THEORY: It is interesting to compare the approximation given by a third order perturbation theory expansion of the type used for large R . Using the formula derived by Dr. Volkoff, (V3) for the frequencies we have tabulated in Table II the values so obtained as compared to the exact solution obtained through a solution of the secular equation for $R = 2.0, 4, 8, 20$. In our case the perturbation formula used for the 5 Zeeman transitions reduces to:

$$\nu_{m \rightarrow m-1} = \nu_0 \left\{ 1 + \frac{2m-1}{2} \lambda + \frac{2^2}{72} c_2(m) \lambda^2 - \frac{2^2}{144} (2m-1) k_2(m) \lambda^3 \right\} \quad (40)$$

$$\text{with } c_2(m) = 4 \left[8 - 6(m - \frac{1}{2})^2 \right]$$

$$k_2(m) = 2 \left[\frac{105}{4} - 5m(m-1) - 6 \right]$$

$$\nu_0 = \frac{2\mu H}{54} = \frac{2eQ\phi_{32}\Gamma}{54} \quad ; \quad \lambda = \frac{3eQ\phi_{32}}{20(\frac{5}{2})\mu H} = \frac{3}{8\Gamma}$$

We have again made use of the value 2.96 Mc/sec for the quadrupole coupling constant. It is seen from Table II that the expansion is certainly valid for $R > 4$.

For all values of $R > 4$, there are no difficulties and the problem is more easily solved by a perturbation expansion of this type. Then only the transitions between adjacent levels are allowed and their frequencies can be calculated with sufficient accuracy by this shorter method.

TABLE I

R	ν_1		ν_2		ν_3	
	ν	$ H_p ^2$	ν	$ H_p ^2$	ν	$ H_p ^2$
0.0	0.000	0.107	0.789	0.243	0.000	0.000
0.4	0.572	0.230	0.623	0.560	0.252	0.014
0.8	1.035	4.064	0.531	5.483	0.371	2.679
1.2	1.190	4.959	0.702	6.983	0.148	3.354
1.6	1.320	5.000	0.861	7.476	0.122	3.562
2.0	1.446	5.011	1.003	7.716	0.392	4.593
2.4	1.569	5.014	1.135	7.830	0.624	6.413
2.8	1.691	5.013	1.261	7.888	0.804	7.809
3.2	1.813	5.013	1.385	7.922	0.948	8.426
3.6	1.935	5.012	1.507	7.940	1.078	8.671
4.0	2.054	5.009	1.627	7.949	1.201	8.784
R	ν_4		ν_5		ν_6	
	ν	$ H_p ^2$	ν	$ H_p ^2$	ν	$ H_p ^2$
0.0	0.758	3.147	0.000	7.014	0.789	4.757
0.4	0.888	2.867	0.035	6.656	0.943	4.727
0.8	0.963	1.112	0.046	5.553	1.195	0.935
1.2	0.789	0.590	0.024	4.364	1.744	0.053
1.6	0.643	1.176	0.021	3.777	2.303	0.030
2.0	0.542	2.304	0.061	3.926	2.840	0.011
2.4	0.504	4.340	0.063	4.590	3.328	0.009
2.8	0.533	6.126	0.009	5.012	3.757	0.007
3.2	0.605	7.030	0.080	5.111	4.146	0.005
3.6	0.698	7.442	0.185	5.109	4.518	0.004
4.0	0.801	7.645	0.297	5.090	4.882	0.003

R	γ_7		γ_8		γ_9	
	ν	$ H'_p ^2$	ν	$ H'_p ^2$	ν	$ H'_p ^2$
0.0	0.758	0.933	1.547	0.005	1.547	0.251
0.4	0.671	1.707	1.259	0.000	1.866	0.124
0.8	0.638	2.921	1.123	1.015	2.204	0.064
1.2	0.664	4.086	1.342	0.857	2.556	0.034
1.6	0.744	4.505	1.626	0.431	2.925	0.018
2.0	0.873	3.800	1.937	0.216	3.321	0.008
2.4	1.066	2.180	2.263	0.115	3.770	0.003
2.8	1.328	0.890	2.598	0.065	4.281	0.001
3.2	1.634	0.354	2.939	0.040	4.832	0.000
3.6	1.961	0.157	3.282	0.025	5.402	0.000
4.0	2.299	0.072	3.629	0.017	5.980	0.000

Transition frequencies (in Mc/sec)
and square of the matrix elements
(arbitrary units) for $0 \leq R \leq 4$, at
intervals of $R = 0.4$.

TABLE II

m	R = 2		R = 4		R = 8		R = 20	
	PVC	Calc.	PVC	Calc.	PVC	Calc.	PVC	Calc.
-5/2	1.43	1.44	2.05	2.05	3.25	3.25	6.80	6.80
-3/2	0.891	1.00	1.67	1.63	2.81	2.81	6.36	6.36
-1/2	0.659	0.392	1.21	1.20	2.38	2.38	5.93	5.93
+1/2	0.293	0.542	0.786	0.800	1.94	1.94	5.48	5.48
+3/2	-	0.061	0.277	0.297	1.47	1.47	5.03	5.03

Frequencies of the Zeeman lines
obtained by a quadrupole inter-
action perturbation theory^(PVC) compared
with the frequencies calculated
directly for the special case of
 $I = 5/2$, $\gamma = 0.95$, $\theta = 0^\circ$, and quad-
rupole constant $C_z = 2.960$ Mc/sec,
for $R = 2, 4, 8$ and 20 .

C. Other orientations of the magnetic field \vec{H}

When the quadrupole energy matrix is written down in a representation in which the xyz axes, to which \vec{I}_x , \vec{I}_y and \vec{I}_z are referred, coincide with the principal axes of the crystal, it has diagonal and $|m - m'| = 2$ non vanishing matrix elements. In a coordinate system that does not coincide with the principal axes, the $|m - m'| = 1$ matrix elements also do not vanish.

The magnetic matrix has only diagonal elements if the axis of quantization of spin coincides with the direction of the magnetic field \vec{H} . Otherwise it has non-vanishing $|m - m'| = 1$ matrix elements as well.

So if, and only if, \vec{H} coincides with any one of the principal axes of the crystal can the $|m - m'| = 1$ matrix elements of both interactions be made to vanish simultaneously. The above analysis (section III, B) is then applicable. For then a "checkerboard" determinant can be obtained from eq. (30) by a simple relabelling of the axes and it splits up into two sub-determinants. For half integral I we have two "races" of eigenvectors of $I + 1/2$ members each. The transitions are possible only between members of different races and we have $(I + 1/2)^2$ lines instead of $I(2I + 1)$.

For example, if the field is along the x-axis, we have to change the definition of A and γ in eq. (30) by the following transformation:

$$A \rightarrow A' = -\frac{A}{2} (1 - \gamma) \quad (41)$$

$$\gamma \rightarrow \gamma' = -\frac{3 + \gamma}{1 - \gamma}$$

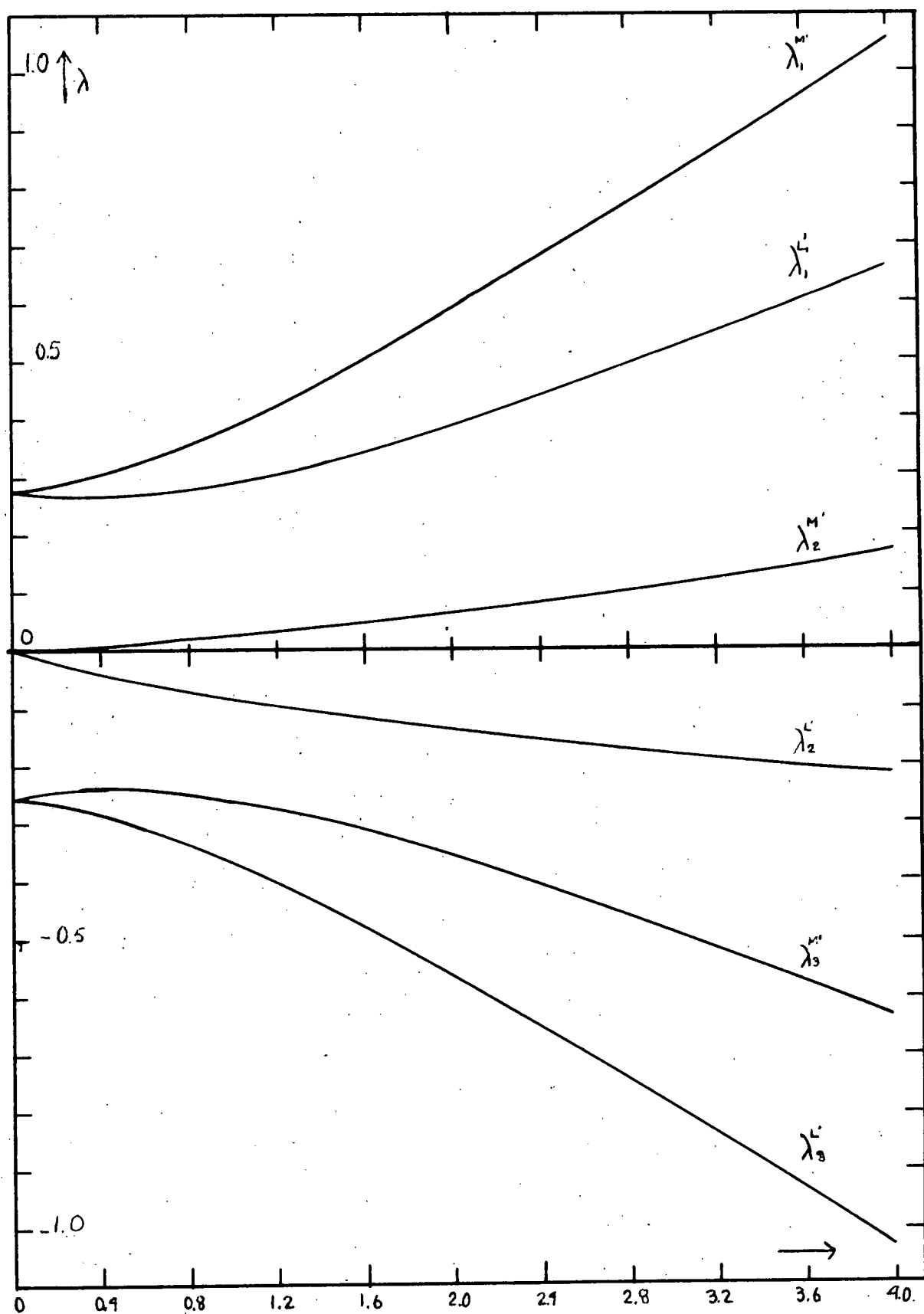


Figure 8. Energy levels for the case $I = 5/2$, $\eta = 0.95$ and $\theta = 90^\circ$ (field along the x-axis) as a function of R .

facing page 39.

The secular determinant is then:

$$\begin{vmatrix} a'' & 0 & h'' & 0 & 0 & 0 \\ 0 & b'' & 0 & j'' & 0 & 0 \\ h'' & 0 & c'' & 0 & j'' & 0 \\ 0 & j'' & 0 & d'' & 0 & h'' \\ 0 & 0 & j'' & 0 & e'' & 0 \\ 0 & 0 & 0 & h'' & 0 & f'' \end{vmatrix} = 0 \quad (42)$$

$$\begin{aligned} \text{where } a'' &= -\frac{1}{8} A(1-\gamma) - \beta - \lambda & d'' &= \frac{1}{10} A(1-\gamma) + \frac{\beta}{5} - \lambda \\ b'' &= \frac{1}{40} A(1-\gamma) - \frac{3}{5}\beta - \lambda & e'' &= \frac{1}{40} A(1-\gamma) + \frac{3}{5}\beta - \lambda \\ c'' &= \frac{1}{10} A(1-\gamma) - \frac{\beta}{5} - \lambda & f'' &= -\frac{1}{8} A(1-\gamma) + \beta - \lambda \\ h'' &= \frac{A}{8\sqrt{10}} (3+\gamma) & j'' &= \frac{3A}{40\sqrt{2}} (3+\gamma) \end{aligned}$$

After rearranging the terms in eq. (42) the secular equations were obtained and solved for $\lambda = \frac{E}{cQq_2}$ as a function of R . The result is given in graphical form in fig. 8. The pattern obtained differs from the one obtained for the field along the z -axis (cf. Fig. 3).

The difference between the two patterns is explained if we realize that the eigenfunctions belonging to the pure quadrupole levels ($R=0$) in this new representation are not nearly pure eigenstates of the spin operator as they were in the previous case (cf. page 30 for the discussion).

Using the transformation matrix to pass from a representation with the axis of quantization along the z -axis to that along the x -axis and the known values of the coefficients of the eigenfunctions for the pure quadrupole levels in the Im_z representation the squares of the coefficients of the angular

momentum eigenfunctions denoted by ψ_{m_x} in the new representation Im_x were found and tabulated in Table III. They can be compared with the squares of the coefficients of the ψ_{m_z} (for $R=0$) in figs. 4 and 5.

TABLE III

	Squares of Coefficients of		
	$\psi_{\frac{5}{2}}$ and $\psi_{\frac{3}{2}}$	$\psi_{\frac{3}{2}}$ and $\psi_{\frac{1}{2}}$	$\psi_{\frac{1}{2}}$ and $\psi_{-\frac{1}{2}}$
HIGHEST LEVEL	0.17	0.51	0.32
MIDDLE LEVEL	0.64	0.00	0.36
LOWEST LEVEL	0.19	0.49	0.32

Squares of the coefficients of the eigenfunctions for the case of the magnetic field along the x-axis, $R=0$.

When the magnetic field is applied along the x-axis, the double degeneracy is removed and we have two classes of eigenfunctions. Class L' consists of $\psi_{\frac{3}{2}}$, $\psi_{\frac{1}{2}}$ and $\psi_{\frac{5}{2}}$ and class M', of $\psi_{-\frac{5}{2}}$, $\psi_{-\frac{3}{2}}$ and $\psi_{-\frac{1}{2}}$. An analysis very similar to the one given in section III, B, can be made. For instance: the state L_1 consists, when $R=0$, of 51% of $\psi_{\frac{3}{2}}$, 31% of $\psi_{\frac{1}{2}}$, and 17% of $\psi_{\frac{5}{2}}$. As R increases $\psi_{\frac{3}{2}}$ will become predominant. When $R \neq 0$ but very small, the corresponding eigenvalue does not increase with R at first. We can visualize the system in this state as being composed of 51% of spins in the $\psi_{\frac{3}{2}}$ state, 31% in $\psi_{\frac{1}{2}}$ and 17% in $\psi_{\frac{5}{2}}$. The Zeeman effect on the spin in state $\psi_{\frac{3}{2}}$ is an increase in energy when R increases and a decrease in energy for the spins in the states $\psi_{\frac{1}{2}}$ and $\psi_{\frac{5}{2}}$. Since we have in all 51% of the first against 49% of the others, the net result is that this

level is almost constant at the start as we can see in fig. 8. But as R increases further, $\psi_{-\frac{3}{2}}$ becomes predominant. In this manner the dependence of the eigenvalue on R can be explained readily.

In this case the gradual change of character of the eigenstates is not so obvious from the energy level diagram of fig. 8, but could be traced easily by drawing graphs similar to those of figs. 4 and 5.

If the r-f field used to investigate the frequency spectrum is placed at right angles to \vec{H} , then, as before, we shall expect only 9 transitions between different classes.

In the most general case when \vec{H} does not coincide with any of the principal axes of the crystal there will always be the $|m - m'| = 1$ non-vanishing matrix elements present no matter what representation is used. The "checkerboard effect" is lost, and all six levels involve all six angular momentum eigenfunctions. Then a $(2I + 1)$ degree equation (cf. eq. (28)) has to be solved, and $(2I + 1)I$ lines are expected with varying intensities. No detailed calculations of this case have been carried out, but the procedure to be followed has been outlined above.

SUMMARY AND CONCLUSION

A complete numerical solution has been obtained for the dependence on the uniform external magnetic field \vec{H} of the expected line frequencies and line intensities for the nuclear resonance transition spectrum^{of Al²⁷} in spodumene for one particular crystal orientation (\vec{H} along one of the principal axes^{of \vec{Q}}).).

At $H = 0$, the pure quadrupole spectrum will consist of two strong lines of almost the same frequency (0.789 and 0.758 Mc/sec) plus a weaker line at the sum of these two frequencies as shown in fig. 6.

As \vec{H} increases, the spectrum gradually changes as shown in fig. 6 or in Table II, until eventually the Zeeman line split into five components by the quadrupole interaction is established. At intermediate fields (around 260 gauss) there is apparently a chance of finding "extra lines", as shown in fig. 6 (γ_8 for $200 < H < 400$ gauss and γ_7 for $100 < H < 750$ gauss).

As long as \vec{H} is along one of the principal axes a maximum of 9 components is possible, although some may be of too low intensity or of too low a frequency to be observed.

If \vec{H} is at an angle to all the principal axes, 15 components become possible in principle, although again some may not be observable for reasons of low intensity or frequency. The complete spectrum can be calculated for any^{crystal} orientation by the method used in this thesis.

REFERENCES

- A1 Allen, J. of Am. Chem. Soc. 74, 6074, 1952.
A2 Andrew and Bersohn, J. Chem. Phys. 18, 159, 1950.
- B1 Bersohn, J. Chem. Phys. 20, 1505, 1952.
B2 Bloembergen, Physica XV, 386, 1949.
B3 Bloembergen, Purcell and Pound, Phys. Rev. 73, 679, 1948.
- C1 Carr and Kikuchi, Phys. Rev. 78, 1470, 1950.
C2 Cohen, Thesis, U. of California, 1952.
C3 Cohen, Bull. Am. Phys. Soc., F.9, Jan. 1953.
- D1 Dean and Pound, J. Chem. Phys., 20, 195, 1952.
D2 Dean, Phys. Rev., 86, 607, 1952.
D3 Dehmelt and Kruger, Naturwiss, 37, 111, 1950.
D4 Dehmelt and Kruger, Naturwiss, 38, 921, 1951.
D5 Dehmelt and Kruger, Z.f. Phys., 129, 401, 1950.
D6 Dehmelt, Z.f. Phys., 130, 356, 1951, and 130, 480, 1951
D7 Dehmelt and Kruger, Z.f. Phys., 130, 385, 1951.
- F1 Feld and Lamb, Phys. Rev., 67, 15, 1945.
- H1 Heitler, "Elementary Wave Mechanics", Oxford, 1945, Pages 118 ff.
- I1 Itoh, Kusaka, Yamagata, Kiriya and Ibamoto,
J. Chem. Phys., 20, 1503, 1952.
- K1 Kruger Z.f. Phys., 130, 371, 1951.
K2 Kruger and Meyer-Berkhout, Z.f. Phys., 132, 171, 1952.
K3 Kruger and Meyer-Berkhout, Z.f. Phys., 132, 221, 1952.
- L1 Livingston, J. Chem. Phys., 20, 1170, 1952.
L2 Livingston, to be published in J. Phys. Chem.
- M1 Meal, J. of Am. Chem. Soc. 74, 6121, 1952.
- P1 Pak, J. Chem. Phys., 16, 327, 1948.
P2 Petch, Volkoff and Cronna, Phys. Rev. 88, 1201, 1952.
P3 Pound, Phys. Rev., 72, 1273, 1948.
P4 Pound, Phys. Rev., 73, 523, 1948.
P5 Pound, Phys. Rev., 73, 1112, 1948.
P6 Pound, Phys. Rev., 79, 685, 1950.
- T1 Townes and Dailey, J. Chem. Phys. 17, 782, 1949, and
20, 35, 1952.
- V1 Van Vleck, Phys. Rev., 74, 1168, 1948.
V2 Volkoff, Petch and Smellie, Can. J. Phys., 30, 270, 1952.
V3 Volkoff and Petch, Cranna and Volkoff, to be published in
Can. J. Phys.

- W1 Watkins and Pound, Phys. Rev., 85, 1062, 1953.
- W2 Waller, Z.f. Phys., 79, 370, 1932.
- W3 Weiss, Phys. Rev., 73, 470, 1948.